Monogenean anchor morphometry: systematic value, phylogenetic signal, and evolution

Tsung Fei Khang, Oi Yoon Michelle Soo, Wooi Boon Tan, Lee Hong Susan Lim

Background. Anchors are one of the important attachment appendages for monogenean parasites. Common descent and evolutionary processes have left their mark on anchor morphometry, in the form of patterns of shape and size variation useful for systematic and evolutionary studies. When combined with morphological and molecular data, analysis of anchor morphometry can potentially answer a wide range of biological questions. **Materials and Methods.** We used data from anchor morphometry, body size and morphology of 13 *Ligophorus* (Monogenea: Ancyrocephalidae) species infecting two marine mugilid (Teleostei: Mugilidae) fish hosts: *Moolgarda buchanani* (Bleeker) and *Liza subviridis* (Valenciennes) from Malaysia. Anchor shape and size data (n=530) were generated using methods of geometric morphometrics. We used 28S rRNA, 18S rRNA, and ITS1 sequence data to infer a maximum likelihood phylogeny. We discriminated species using principal component and cluster analysis of shape data. Adams's K_{mult} was used to detect phylogenetic signal in anchor shape. Phylogeny-correlated size and shape changes were investigated using continuous character mapping and directional statistics, respectively. We assessed morphological constraints in anchor morphometry using phylogenetic regression of anchor shape against body size and anchor size. Anchor morphological integration was studied using partial least squares method. The association between copulatory organ morphology and anchor shape and size in phylomorphospace was used to test the Rohde-Hobbs hypothesis. We created monogeneaGM, a new R package that integrates analyses of monogenean anchor geometric morphometric data with morphological and phylogenetic data. **Results**. We discriminated 12 of the 13 *Ligophorus* species using anchor shape data. Significant phylogenetic signal was detected in anchor shape. Thus, we discovered new morphological characters based on anchor shaft shape, the length between the inner root point and the outer root point, and the length between the inner root point and the dent point. The species on *M. buchanani* evolved larger, more robust anchors; those on *L. subviridis* evolved smaller, more delicate anchors. Anchor shape and size were significantly correlated, suggesting constraints in anchor evolution. Tight integration between the root and the point compartments within anchors confirms the anchor as a single, fully integrated module. The correlation between male

copulatory organ morphology and size with anchor shape was consistent with predictions from the Rohde-Hobbs hypothesis. **Conclusions.** Monogenean anchors are tightly integrated structures, and their shape variation correlates strongly with phylogeny, thus underscoring their value for systematic and evolutionary biology studies. Our MonogeneaGM R package provides tools for researchers to mine biological insights from geometric morphometric data of speciose monogenean genera.

1 Running head: ANCHOR MORPHOMETRY FOR MONOGENEAN SYSTEMATICS

2 Title: Monogenean anchor morphometry: systematic value, phylogenetic signal, and evolution

3 Authors: Tsung Fei Khang[1*], Oi Yoon Michelle Soo[2], Wooi Boon Tan[3], Lee Hong Susan Lim[2+]

4 *[1]Institute of Mathematical Sciences, Faculty of Science, University of Malaya, 50603 Kuala*

5 *Lumpur, Malaysia.*

6 *[2]Institute of Biological Sciences, Faculty of Science, University of Malaya, 50603 Kuala Lumpur,*

7 *Malaysia.*

8 *[3]Centre for Tropical Biodiversity Research, University of Malaya, 50603 Kuala Lumpur,*

9 *Malaysia.*

10 *Corresponding author

11 +Deceased on 2 August 2014

12 Email: tfkhang@um.edu.my

13 Tel: +603 79674171

14 Fax: +603 79674143

15 ABSTRACT

16 **Background.** Anchors are one of the important attachment appendages for monogenean

17 parasites. Common descent and evolutionary processes have left their mark on anchor

18 morphometry, in the form of patterns of shape and size variation useful for systematic and

19 evolutionary studies. When combined with morphological and molecular data, analysis of anchor

20 morphometry can potentially answer a wide range of biological questions.

21 **Materials and Methods.** We used data from anchor morphometry, body size and morphology of

22 13 *Ligophorus* (Monogenea: Ancyrocephalidae) species infecting two marine mugilid (Teleostei:

23 Mugilidae) fish hosts: *Moolgarda buchanani* (Bleeker) and *Liza subviridis* (Valenciennes) from

24 Malaysia. Anchor shape and size data (n=530) were generated using methods of geometric

25 morphometrics. We used 28S rRNA, 18S rRNA, and ITS1 sequence data to infer a maximum

26 likelihood phylogeny. We discriminated species using principal component and cluster analysis of

27 shape data. Adams's K_{mult} was used to detect phylogenetic signal in anchor shape. Phylogeny-

28 correlated size and shape changes were investigated using continuous character mapping and

29 directional statistics, respectively. We assessed morphological constraints in anchor morphometry

30 using phylogenetic regression of anchor shape against body size and anchor size. Anchor

31 morphological integration was studied using partial least squares method. The association

32 between copulatory organ morphology and anchor shape and size in phylomorphospace was used

33 to test the Rohde-Hobbs hypothesis. We created `monogeneaGM`, a new R package that integrates

34 analyses of monogenean anchor geometric morphometric data with morphological and

35 phylogenetic data. **Results.** We discriminated 12 of the 13 *Ligophorus* species using anchor shape

36 data. Significant phylogenetic signal was detected in anchor shape. Thus, we discovered new

37 morphological characters based on anchor shaft shape, the length between the inner root point

38 and the outer root point, and the length between the inner root point and the dent point. The

39 species on *M. buchanani* evolved larger, more robust anchors; those on *L. subviridis* evolved

40 smaller, more delicate anchors. Anchor shape and size were significantly correlated, suggesting

41   constraints in anchor evolution. Tight integration between the root and the point compartments

42   within anchors confirms the anchor as a single, fully integrated module. The correlation between

43   male copulatory organ morphology and size with anchor shape was consistent with predictions

44   from the Rohde-Hobbs hypothesis. **Conclusions.** Monogenean anchors are tightly integrated

45   structures, and their shape variation correlates strongly with phylogeny, thus underscoring their

46   value for systematic and evolutionary biology studies. Our MonogeneaGM R package provides

47   tools for researchers to mine biological insights from geometric morphometric data of speciose

48   monogenean genera.

49   Keywords: cluster heat map - geometric morphometrics - *Ligophorus* - molecular phylogeny -

50   Monogenea – morphological integration – phylogenetic regression - phylomorphospace -

51   principal component analysis – shape and size variation

52   INTRODUCTION

53   The Monogenea is a class of flatworms (Platyhelminthes) that are primarily ectoparasites

54   of fish (Whittington, 2005; Hayward, 2005). An adult monogenean parasite has well-developed

55   attachment appendages located at its anterior (prohaptor) and posterior (opisthaptor) regions that

56   help it to resist physical dislodgement from the host. The posterior attachment organs consist of

57   sclerotized hard parts such as hooks, anchors and clamps. Ecologically, monogenean parasites are

58   characterized by their strong host specificity

59   (Whittington et al., 2000). The Monogenea has several desirable features that make it invaluable

60   as a model system for studying evolutionary processes that resulted in its past diversification and

61   present diversity (Poulin, 2002). Primarily, many of its genera are speciose, morphologically

62   diverse, show well-resolved phylogenies at the familial level (Boeger and Kritsky, 1997, 2001;

63   Mollaret et al., 2000), and samples can be easily obtained in large numbers. It has been used as a

64   model to shed light on ecological forces that shape species community and structure (Rohde,

65   1979; Mouillot et al., 2005; Raeymaekers et al., 2008), to investigate processes leading to

66   speciation and its maintenance (Rohde and Hobbs, 1986; Rohde 1994; de Meeus et al., 1998;

67   Šimková et al., 2002; Hahn et al., 2015; Vanhove and Huyse, 2015), to elucidate host-parasite

68   evolutionary ecology (Desdevises et al., 2002; Huyse et al., 2003; Huyse and Volckaert, 2005;

69   Šimková et al., 2006; Šimková and Morand, 2008; Mendlová and Šimková, 2014; Grégoir et al.,

70   2015), and to explore the extent of correlation between phenotype variation in attachment organs

71   and factors such as phylogeny, host specificity and geographical location (Vignon et al., 2011).

72   Morphometric variation in anatomical structures of interest can be studied using two

73   approaches. Traditional morphometrics (Reyment et al., 1984; Marcus, 1990) is characterized by

74   the use of lengths of defined positions on anatomical structures of interest (or their ratios) as

75   input data for multivariate statistical analyses. While such variables may measure size adequately,

76   they are generally not effective for capturing shape information present in the geometry of a set

77   of defined points of an object (Rohlf and Marcus, 1993). A large proportion of biological

78   variation due to shape differences is therefore missed when an analysis uses only information

79   from variation in length variables.

80   With the development of geometric morphometrics over the past three decades,

81   researchers now have, at their disposal, a powerful method for extracting, visualizing and

82   combining shape data with other data types such as molecular phylogenies to attain an integrative

83   evolutionary analysis (Rohlf and Marcus, 1993; Adams et al., 2004; Adams et al., 2013).

84   Digitization of the anatomical structure of interest provides the key to the acquisition and use of a

85   new type of data - landmark coordinates, from which shape information can be effectively

86   extracted, and then analyzed, using new tools such as Procrustes superimposition, thin plate

87   splines, relative warp analysis and elliptic Fourier analysis. Geometric morphometrics is now

88   commonly used in systematics and evolutionary biology research where analysis of shape can be

89   expected to provide new insights to complement traditional morphometric, phylogenetic or

90   biogeographic analyses. A cursory search in major biological journal databases for recent

91   publications having "geometric morphometrics" in their keywords revealed that geometric

92   morphometrics is widely used to study various biological aspects, in diverse phyla, such as fish

93   taxonomy (Sidlauskas et al., 2011), plant taxonomy (Conesa et al., 2012), gastropod shell shape

94   variation (Smith and Hendricks, 2013; Cruz et al., 2012), morphological adaptation in birds

95   (Sievwright and MacLeod, 2012), fly wing evolution (Pepinelli et al., 2013), turtle neck shape

96   evolution (Werneburg et al., 2015), beetle speciation (Pizzo et al., 2013) and species boundary

97   problems in butterflies (Barão et al., 2014). Because of the inherently digital nature of geometric

98   morphometric data, its increasing prominence in morphological studies accentuates the role of

99   informatics in modern taxonomy (Wheeler, 2007).

100   In morphological analyses of monogeneans, taxonomists often prioritize prominent

101   sclerotized parts such as the copulatory organ, because qualitative variation in the latter is

102   frequently sharp and easy to describe. Nonetheless, morphometric variation in all sclerotized

103   parts of monogeneans has been studied for a long time from the perspective of systematics (e.g.

104   Shinn et al., 2001) and evolutionary ecology (e.g. Poisot and Desdevises, 2010; Mendlová and

105   Šimková, 2014). Hard parts such as the anchors are ideal for geometric morphometric analysis

106   because they are not easily deformed by compression when mounted onto slides (Lim and

107   Gibson, 2009). Anchor shape and size are taxonomically informative. Typically, size information

108   is captured quantitatively in the form of distances between two defined -points on the anchors,

109   and shape information is captured qualitatively in the form of character states. The analysis of

110   monogenean morphometric data has been, and continues to be, dominated by the application of

111   traditional morphometrics (e.g. Mariniello et al., 2004; Shinn et al., 2004; Tan et al., 2010; Hahn

112   et al., 2011; Soo and Lim, 2012). To date, there are only few examples (Vignon and Sasal, 2010;

113   Vignon, 2011; Vignon et al., 2011; Rodríguez-González et al., 2015a) of applying geometric

114   morphometrics to analyze monogenean anchor shape variation to overcome the limitations in

115   data resolution inherent in standard morphometric and qualitative analyses. The paucity of

116   geometric morphometric studies, however, belies the importance of this approach in uncovering

117   intraspecific shape variation in anchors that can be invaluable for species delimitation,

118   particularly in resolving synonymyiess (e.g. Pérez Ben et al., 2014), as well as for testing

119   hypotheses of morphological integration (Olson and Miller, 1958) and evaluating levels of

120   phenotypic plasticity (Pfennig et al., 2010).

121   As anchors serve a functional purpose, a priori, it is unclear whether phenotypic similarity

122   of anchors among species is an outcome of adaptive processes related to the ecology or the

123   morphology of their fish host, or simply a reflection of their phylogenetic constraint (Morand et

124   al., 2002). If the presence of phylogenetic signal in anchors can be statistically established,

125   evolutionary analysis of shape and size change can then be used to elucidate trends in particular

126   clades. The results are expected to be useful for guiding the selection of appropriate anchor

127   morphometric variables for conversion into morphological characters that have lower levels of

128   homoplasy, thus overcoming the problem of unnecessary homoplasy of a morphological

129   character arising from poor quality and insufficient number of character states (Perkins et al.,

130   2009).

131   In this paper, we developed an integrative analysis that uses data from anchor

132   morphometry and morphology, as well as DNA sequences, that allows the investigation of broad

133   aspects in the systematic biology of monogeneans, such as species discrimination, evolutionary

134   ecology, phylogenetic signal, and morphological integration. For illustration, we used data

135   obtained from 13 recently described species belonging to the *Ligophorus* (Monogenea:

136 Ancyrocephalidae) genus, a particularly speciose genus with 63 species known to date (Table

137 S1). Thus, our study covered all the *Ligophorus* species (approximately 20% of global

138 *Ligophorus* diversity) currently found on two mullet host species in Southeast Asia. Mullets are

139 eaten by people in this region.

140 MATERIALS AND METHODS

141 *Samples*

142 We obtained 530 specimens (metadata in Table S2; sample sizes in Table S3) belonging to

143 13 *Ligophorus* species (Soo and Lim, 2012; Soo and Lim, 2015; Soo et al., 2015) from two

144 species of adult ~~fish~~ mullet host: *Liza subviridis* Valenciennes, 1836 (n=52) and *Moolgarda*

145 *buchanani* Bleeker, 1853 (n=29) from several locations in tropical Western Peninsular Malaysia

146 (Fig. S1). The specimens have been deposited in the Museum of Zoology at University of

147 Malaya (508 specimens), the Natural History Museum, London (14 specimens), and the Lee

148 Kong Chian Natural History Museum, Singapore (6 specimens).

149 From 2009 to 2014, *Liza subviridis* was collected off Carey Island in Selangor (2º 52' N,

150 101º 22' E), and *M. buchanani* off Langkawi Island in Kedah (6° 21' N, 99° 48' E) and the sea off

151 Johor (1° 20′N, 103° 32′ E). The fish were obtained from local fishermen in the vicinity of the

152 sampling locations, dead at the time of purchase. Seven of the 13 species: *L. bantingensis* Soo &

153 Lim, 2012, *L. careyensis* Soo & Lim, 2012, *L. chelatus* Soo & Lim, 2012, *L. funnelus* Soo &

154 Lim, 2012, *L. navjotsodhii* Soo & Lim, 2012, *L. parvicopulatrix* Soo & Lim, 2012 and *L.*

155 *belanaki* Soo & Lim, 2015 were found on *Liza subviridis*; the remainder: *L. fenestrum* Soo &

156 Lim, 2012, *L. kedahensis* Soo & Lim, 2012, *L. kederai* Soo & Lim, 2015, *L. grandis* Soo, Tan &

157 Lim, 2015, *L. johorensis* Soo, Tan & Lim, 2015, and *L. liewi* Soo, Tan & Lim, 2015, were found

158 on *M. buchanani*. For all 81 fish examined, the *Ligophorus* species found in *M. buchanani* were

159 never observed in *Liza subviridis*, and vice versa.

160   When preparing slides, we used a basic mounting protocol (Lim, 1991) where the

161   monogeneans were put onto a clean slide with a drop of water, and then covered with a coverslip.

162   Specimens were initially mounted in modified ammonium picrate glycerine, and subsequently

163   converted into unstained, permanent mounts in Canada balsam. The opisthaptorial sclerotized

164   hard parts of *Ligophorus* consist of a pair (left and right) of dorsal and ventral anchors, bars, and

165   marginal hooks. Digital images of these hard parts were taken from labelled mounted slides using

166   a light microscope with Leica digital camera (DFC 320) connected to the QWin plus image

167   analysis software (Leica Microsystems, Germany) under 40x magnification, saved as jpeg files

168   and organized into folders. Three species

169   (*L. fenestrum*, *L. liewi* and *L. kederai*) showed a probable fixed character state – that of the

170   presence of fenestrated structures on anchors of all examined specimens, since no variation in this

171   character state was observed in all examined specimens of these three species.

172   *Data Acquisition*

173   Where possible, we measured a specimen's body length from its anterior to posterior end,

174   and body width at the midpoint of its body. To obtain landmark coordinate data from the anchors,

175   we used TPSDIG2 (Rohlf, 2013; Rohlf, 2015). Eleven landmarks (LM; six Type I, five Type III)

176   were placed sequentially on the right and left ventral and dorsal anchors of each specimen (Fig.

177   1).

a) b)

178   FIGURE 1.
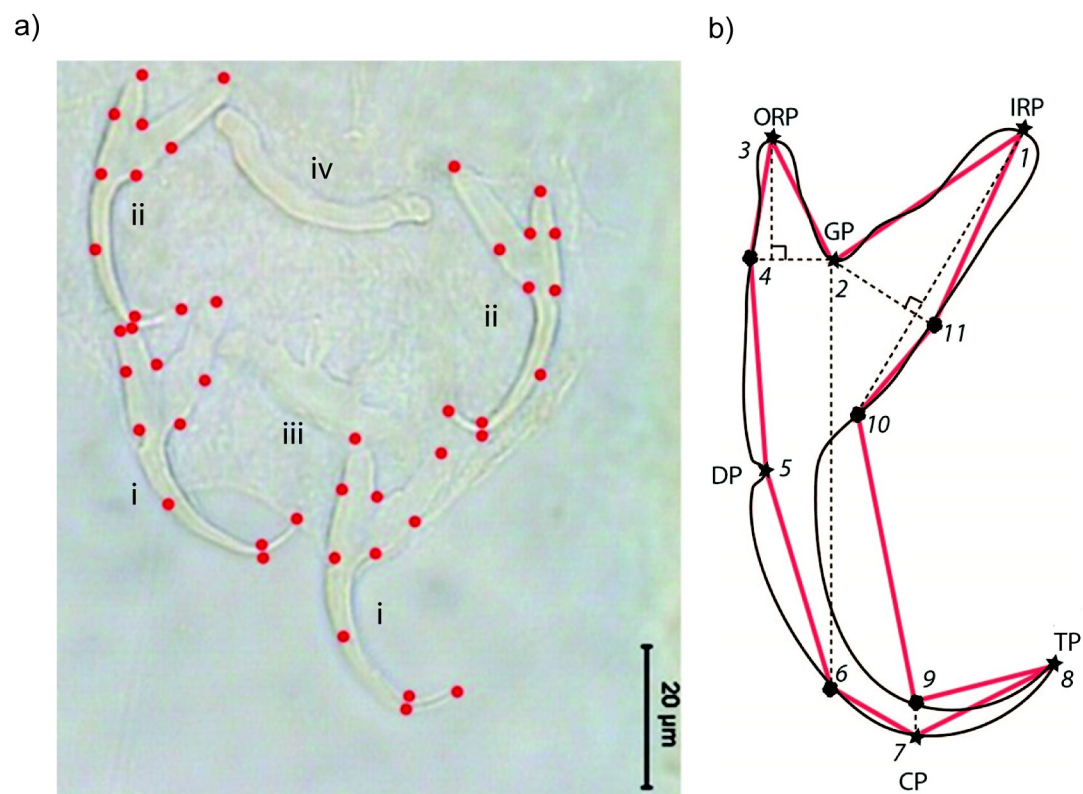
179   The set of all 11 landmark coordinates makes up a specimen's landmark configuration.

180   Six of the landmarks are Type I (LM1,LM2,LM3,LM5,LM7,LM8), while the remainder

181   (LM4,LM6,LM9,LM10,LM11) are Type III (i.e. semi-landmarks). LM1and LM3 are the inner

182   root point and the outer root point, respectively. Sandwiched between them is LM2, the groove

183   point. LM5 is the dent point, while LM7 is the curve point. The tip point is represented by LM8.

184   The semi-landmarks were defined relative to Type I landmarks. The horizontal (towards the outer

185   root point) and vertical projections (towards the curve point) from LM2 intersect with the anchor

186   outline to give LM4 and LM6, respectively. LM9 and LM10 are the intersection points between

187   the vertical projection from LM7 and LM1 with anchor outline, respectively. The projection from

188   LM2 perpendicular to the vertical projection from LM1 touches the anchor outline to define

189   LM11. We used the set of landmarks LM1 to LM4 and LM11 to represent the shape of the root

190   compartment, and the set LM5 to LM10 to represent the point compartment. For geometric

191   morphometric analysis, semi-landmarks were not specially treated (e.g. employing sliding

192   landmark analysis), following MacLeod (2013) that such treatments may introduce distortions to

193   the original geometrical relationship that lead to complicated interpretations of the result. The

194   anchor images and their corresponding landmark coordinate data are given in Supplemental

195   Material D1 and D2, respectively.

196   *Data Processing and Analysis Tools*

197   We created a new R (Version 3.2.1; R Core Team, 2015) package called `monogeneaGM`

198   (Khang, 2015) to process raw landmark coordinate data and integrate new methodological

199   developments in the current study with numerous data processing and analysis tools in R

200   packages, such as `geomorph` (Adams and Otarola-Castillo, 2014), `phytools` (Revell, 2012),

201   `circular` (Agostinelli and Lund, 2013), `gplots` (Warnes et al., 2014), `ape` (Paradis et al.

202   2004), `rgl` (Adler et al., 2014) and `cluster` (Maechler et al., 2015).

203   The `monogeneaGM` package contains a suite of R functions for three primary analyses:

204   anchor landmark coordinate data quality control, visual checks and Generalized Procrustes

205   Analysis; hierarchical clustering and principal component analysis; and analysis of anchor shape

206   change using directional statistics. Some of the functions are suitable for general use. For

207   example, the phylomorphospace visualization functions - `tpColorPlot2d` for two-

208   dimensional data, and `tpColorPlot3d` for three-dimensional data, can take in two additional

209   arguments: a color transparency control, which is useful for improving graphical presentation

210   when there are substantial overlaps of data points, and an option to superimpose a user-supplied

211   phylogeny onto defined centroids in the scatter plot, if this information is available.

212   *Data Quality Control*

213   Despite careful slide preparation, it is inevitable that anchor images of some specimens

214   would contain substantial amount of non-biological shape variation caused by incongruent image

215   and object planes (Arnqvist and Mårtensson, 1998). The inclusion of these poor quality data in

216   downstream analyses is undesirable, as they introduce noise into an analysis that can potentially

217   complicate the interpretation of results. To mitigate this problem, we developed a quality control

218   procedure to filter out poor quality images. In this procedure, we first computed all pairwise

219   Euclidean distances between landmarks for the left and right forms of dorsal and ventral anchors.

220   If both left and right forms have congruent image and object planes, then by symmetry, their

221   residual – the difference of their pairwise Euclidean distances for each landmark (M), should be

222   close to zero, thus yielding a small sum of squared residuals (M^2). Moreover, we expect M to be

223   randomly distributed with zero mean across all average pairwise Euclidean distances (A) between

224   the left and right forms. The slope of the regression equation of M against A (b) allows us to

225   measure how well this expectation is satisfied. To be comparable with the sum of squared

226   residuals, we squared the estimated regression slope (b^2), and then scaled it to be on the same

227   order of magnitude as M^2. Thus, a good quality specimen would have small sum of M^2 and b^2,

228   and vice versa. We defined the quality score Q, as

$$Q = 100 \times 10^{\frac{-\sqrt{M^2+b^2}}{10}}$$

229   .

230   The magnitude of this measure is straightforward to interpret – it is high (maximum 100) for

231   good quality specimens and low (minimum 0) for poor ones. Figure 2 shows examples of poor

232   and good quality specimens together with their Tukey Mean-Difference (TMD) plots,

233   respectively. Specimens with Q of 10 or more (n=437; Table S3 and Fig. S2) were used for

234   subsequent analyses.

a)

b)

235   FIGURE 2.
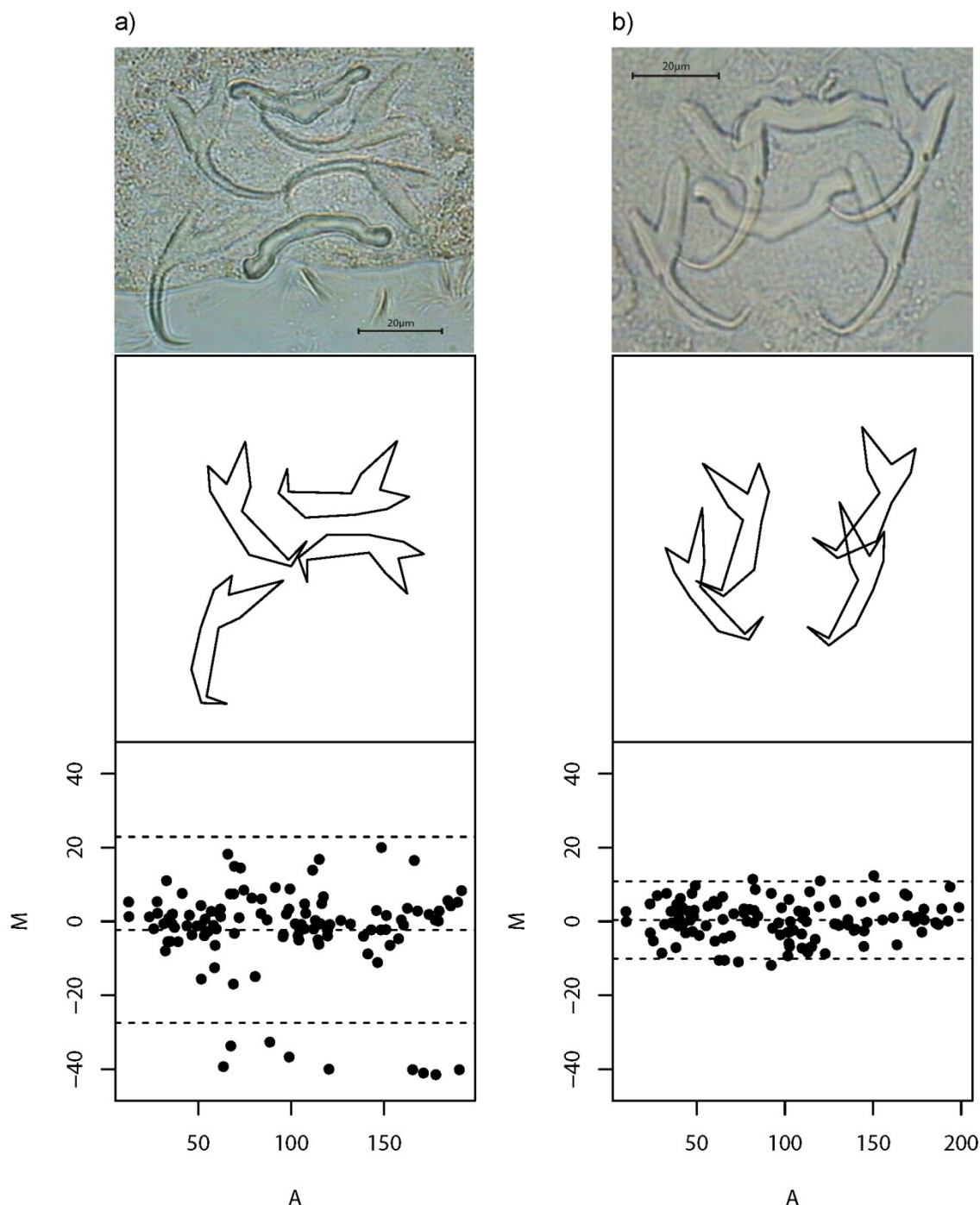
236   *Converting Pairwise Euclidean Distances in Arbitrary Units to Physical Units*

237   We used a subset (n=96) of the total specimens with quality score above 10 (n=437) and

238   measured the physical distances from LM1 to LM3 and from LM1 to LM5 in these samples

239   using QWin plus image analysis software (Leica Microsystems, Germany). We then regressed the

240   physical distances against the computed pairwise Euclidean distances to determine the linear

241   equation for converting arbitrary distance units into their physical units (in μm). Thus, all

242   pairwise Euclidean distances computed from raw landmark coordinates could be converted to

243   physical distances by multiplication with a factor of 0.2 followed by addition of 0.9 (Fig. S3).

244   *Geometric Morphometric Analysis*

245   For each species, we performed Generalized Procrustes Analysis (GPA; Gower, 1975;

246   Rohlf and Slice, 1990) to align the sample landmark configurations for both ventral and dorsal

247   anchors, using the `gpagen` function in the `geomorph` package (Version 2.1.1; Adams and

248   Otarola-Castillo, 2014). The resulting GPA coordinates of the left and right forms were then

249   averaged. GPA removes the effects of translation, rotation and scaling so that the resulting

250   landmark configurations have minimum sum of squared distances with respect to the mean

251   landmark configuration (Adams et al., 2004). Nevertheless, even after GPA, comparison of

252   anchor shape variation can still be potentially confounded by the presence of non-biological

253   variation in the landmark configuration. Specifically, if many samples of a species have anchors

254   lying in one particular position, it would not be clear whether variation between its members'

255   mean GPA landmark configuration and those of other species constitutes genuine biological

256   variation or mathematical artifact. Typical application of geometric morphometrics in non-

257   microscopic objects (fly wings, skulls, etc.) does not usually suffer from this problem, since

258   specimens from species to be compared can be manipulated into standardized positions before

259   imaging.

260   To ensure that the landmark configurations of all 13 species were comparable, we

261   determined the angular deviation of LM7 from the $x=0$ line, and rotated all landmark coordinates

262   by this amount with the origin as pivot. This has the effect of creating standardized landmark

263   configurations for specimens across all species since the x-coordinate of LM7 is always zero after

264   adjustment. The GPA coordinate data of all specimens thus obtained were subjected to another

265   iteration of GPA to produce the final shape alignment, which was organized into a data matrix

266   with rows representing specimens and columns representing the 44 GPA landmark coordinates.

267   *Molecular Phylogenetic Analysis*

268   We used DNA sequence data from three nuclear markers: 28S rRNA, 18S rRNA and ITS1

269   from the 13 *Ligophorus* species to infer their phylogenetic tree. These markers are a mainstay of

270   parasitic platyhelminth molecular phylogenetics (Littlewood, 2008), and the combination of fast

271   (ITS-1) and slow (28S rRNA, 18S rRNA) evolving sequences should provide sufficient

272   resolution for the inferred phylogenetic tree (Lockyer et al., 2003; Blair, 2006; Waeschenbach et

273   al., 2007), allowing the relationship of even closely related monogenean species to be resolved

274   (e.g. in *Gyrodactylus* (Gilmore et al., 2012)). Ideally, the inclusion of mitochondrial markers such

275   as cytochrome oxidase I (COI) would provide a more representative sampling of the genome, and

276   hence, a more reliable phylogeny. However, the absence of mitochondrial data may not impact

277   the quality of the inferred phylogeny, since, for monogeneans, it has been shown in Diplectanidae

278   and *Gyrodactylus* that both rRNA and mitochondrial markers are effective for species

279   identification (Vanhove et al., 2013). Regardless of whether nuclear or mitochondrial genes are

280   used, it is important to keep in mind that gene trees do not always reflect the species tree

281   (Maddison, 1997).

282   Partial 28S rRNA (~800bp) and ITS1 (~750bp) sequence data were obtained from Soo et

283   al. (2015), whereas 18S rRNA sequence data were generated in the present study. Briefly, the

284   *Ligophorus* specimens were removed from host gills, identified morphologically and then

285   preserved in 75% ethanol. Genomic DNA was extracted from samples using DNAEasy extraction

286   kit (QIAGEN, Hilden, Germany). About 5µl of the extracted DNA was used as template in the

287   PCR reaction to amplify the partial 18S rRNA sequence using two primers: WormA (5'-

288 GCGAATGGCTCATTAAATCAG-3') (Littlewood and Olson, 2001) and new930F (5'-

289 CCTATTCCATTATTCCATGC-3') (modified from Littlewood and Olson, 2001). The PCR

290 reaction (50μl) was carried out in a solution containing 1.5mM MgCl$_2$, PCR buffer (Fermentas),

291 200μM of each deoxyribonucleotide triphosphate, 1.0 μM of each PCR primer and 1U of Taq

292 polymerase (Fermentas), in a thermocycler (Eppendorf Mastercycler) using the following

293 conditions: initial denaturation at 95°C for 4 minutes, followed by 35 cycles of 95°C, 52°C and

294 72°C for one minute each, with final extension at 72°C for 10 minutes. An aliquot (10μl) from

295 the amplicons were electrophoresed in 1.3% agarose gel, stained with ethidium bromide and

296 viewed under an ultraviolet illuminator. The remaining 40μl of each amplicon was purified using

297 a DNA purification kit (QIAGEN, Hilden, Germany) and subjected to automated DNA

298 sequencing (ABI 3730 DNA Sequencer, First Base Laboratories, Kuala Lumpur) using the same

299 primers used for PCR amplification. Approximately 750 bp of the 18S rRNA sequence were

300 amplified and sequenced for the 13 *Ligophorus* species (Table 1).

Ligophorus species	Host species	Locality (Malaysia)	GenBank Accession no.		
			28S rRNA	18S rRNA	ITS1

L. bantingensis	*Liza subviridis*	Carey Island, Selangor	KM221909	KM221934*	KM221922
L. belanaki			KM221910	KM221935*	KM221923
L. careyensis			KM221911	KM221936*	KM221924
L. chelatus			KM221912	KM221937*	KM221925
L. funnelus			KM221914	KM262663*	KM262662
L. navjotsodhii			KM221920	KM221944*	KM221932
L. parvicopulatrix			KM221921	KM221945*	KM221933
L. fenestrum	*Moolgarda buchanani*	Langkawi Island, Kedah	KM221913	KM221938*	KM221926
L. kedahensis			KM221917	KM221941*	KM221929
L. kederai			KM221918	KM221942*	KM221930
L. grandis		Straits of Johor	KM221915	KM221939*	KM221927
L. johorensis			KM221916	KM221940*	KM221928
L. liewi			KM221919	KM221943*	KM221931

301   TABLE 1.

302   For phylogenetic analysis, we first aligned sequences for each marker using MAFFT

303   (Version 7 at http://mafft.cbrc.jp/alignment/server/; Katoh and Standley, 2013). The alignment

304   parameters used were the Q-INS-i iterative refinement method, the 1PAM/κ=2 nucleotide scoring

305   matrix with a gap opening penalty of 1.53. We then concatenated multiple sequence alignments

306   of the three nuclear markers (28S rRNA-ITS1-18S rRNA). The resulting supermatrix was used as

307   input in IQ-TREE (Nguyen et al. 2015) to construct the maximum likelihood (ML) phylogenetic

308   tree (Felsenstein, 1981; Felsenstein, 2003). IQ-TREE is a state-of-the-art ML tree construction

309   pipeline that integrates DNA model selection, maximum likelihood tree search, and rapid

310   bootstrap analysis (Minh et al., 2013). For model selection, we used the Bayesian Information

311   Criteria, and did not consider "G+I" models, following Yang (2006) that modelling proportion of

312   invariable sites in the presence of gamma rate variation across sites creates model identifiability

313   issues. MEGA (Version 6; Tamura et al., 2013) was used to edit the resulting phylogenetic tree.

314   We annotated the tree with the morphology of anchors, bars and male copulatory organ to allow

315   visual assessment of overall phylogenetic and phenotypic correlation.

316   *Species Discrimination*

317   Discriminating a monogenean species is a complex art that involves the comparison of

318   qualitative features of numerous anatomical structures: the male copulatory organ, female

319   reproductive organ, anchors, bars and marginal hooks. Among the sclerotized hard parts,

320   multivariate morphometric analyses of shape and size variables of suitable anatomical structures

321   provide a quantitative means for species discrimination, which is invaluable for complementing

322   the results from qualitative morphological analyses.

323   To visualize species clustering in low dimension morphospace, we applied Principal

324   Component Analysis (PCA) separately for the ventral and dorsal anchors using their GPA

325   coordinate data. The trade-off between loss of information through dimensional reduction and

326   gain of interpretation via visualization in PCA can, however, make it difficult to judge how well

327   members of the same species cluster together in the PCA scatter plots, especially when there are

328   overlaps between different species clusters. To overcome this problem, we complemented PCA

329   results with the cluster heat map (Wilkinson and Friendly, 2008), a powerful method for

330   organizing high-dimensional multivariate data that allows visual detection of patterns of

331   variation. The cluster heat map first maps numerical information in the cells of the input data

332   matrix to corresponding color codes. Then, a hierarchical clustering algorithm is applied to

333   cluster the samples by similarity, in such a way that within cluster variation is always smaller

334   than between cluster variation. For the current analysis, we estimated similarity between each

335   pair of samples using the Manhattan distance metric. The resulting distance matrix was then used

336   as input for hierarchical clustering of samples using the Ward algorithm.

337   To assess the impact of applying the quality control procedure, we compared cluster heat

338   maps generated using all samples, and using only samples that passed data quality control. Heat

339   map construction was done using the `heatmap.2` function in the `gplots` package (Version

340   2.13.0; Warnes et al., 2014). We found the simple heat map a good alternative to inspection of the

341   PC loadings table when trying to interpret the first few PC axes biologically.

342   *Testing for the Presence of Phylogenetic Signal in Anchor Shape*

343   Species with different shapes are localized in particular regions of the morphospace.

344   When a phylogeny is superimposed onto this morphospace, a phylomorphospace is induced, and

345   it becomes possible to evaluate whether common descent or convergent evolution is likely to

346   have shaped phenotypic similarity (Klingenberg and Ekau, 1996; Sidlauskas, 2008; Revell,

347   2014). If anchor shape contains substantial phylogenetic signal, then we expect the phylogeny to

348   have non-random branching patterns in phylomorphospace. Graphically, we may visualize the

349   latter by superimposing the molecular phylogeny of *Ligophorus* on the PCA plots of the first

350   three principal components for the ventral and dorsal anchors. Estimation of ancestral node

351   positions in the phylomorphospace was done using the maximum likelihood method as

352   implemented in the `fastAnc` function of the `phytools` package (Version 0.4-21; Revell,

353   2012).

354   We formally tested the presence of phylogenetic signal in anchor shape by applying

355   Adams's multivariate K_{mult} test (Adams, 2014a), implemented using the `physignal` function

356   (10 000 iterations) in the `geomorph` package (Version 2.1.1; Adams and Otarola-Castillo, 2013).

357   The K_{mult} statistic is a multivariate generalization of Blomberg's K statistic (Blomberg et al.,

358   2003). The phenotype (a continuous trait) interest in the lineages of a given phylogeny is

359   assumed to evolve in phylomorphospace according to Brownian motion. In the absence of

360   phylogenetic signal, $K_{mult} = 0$ (i.e. phenotypic variation is independent of lineages). At $K_{mult} = 1$,

361   phenotypic variation between taxa in the same lineage conforms to expectation under Brownian

362   motion evolution. Values of $K_{mult} < 1$ correspond to phenotypic variation that is larger than

363   expected between taxa of the same lineage, and values of $K_{mult} > 1$ correspond to phenotypic

364   variation that is smaller than expected between taxa of the same lineage (Adams, 2014a).

365   Statistical significance is determined via a permutation procedure under assumption of

366   phylogenetic signal absence.

367   *Analysis of Anchor Shape and Size Evolution*

368   In studying anchor shape and size evolution, we were primarily concerned with trends

369   occurring in different clades of the phylogeny of the 13 *Ligophorus* species. To control for the

370   effect of body size in subsequent phylogenetic regression analysis of anchor shape against anchor

371   size, it was necessary to first test for collinearity of body size and anchor size (Mundry, 2014).

372   Since body size was prone to distortion during fixation, we used the median of body length and

373   body width of each species to reduce the impact of outliers. For analysis, the logarithm (base 10)

374   of the product of median body length and median body width was used.

375   The GPA landmark coordinates of the ancestral anchor were estimated using the

376   maximum likelihood method as implemented in `fastAnc` function from the `phytools`

377   package (Version 0.4-21; Revell, 2012) . Anchor shape change associated with a clade is

378   statistically supported if mean directional change deviates significantly from uniformity in a set

379   of landmarks. We visualized directional deviation in the 11 landmarks of both ventral and dorsal

380   anchors using circular plots (Agostinelli and Lund, 2013; implemented in the `circular`

381   package, Version 0.4-7). We then performed Rayleigh's test (Batschelet, 1981) to test for

382   evidence against directional uniformity in each landmark. The strength of statistical evidence

383   against mean directional uniformity in each landmark was assessed using p-value. Wireframe-

384   lollipop plots (Klingenberg, 2013) were used to graphically summarize the mean change in

385   direction and mean magnitude of landmark displacement from root ancestor landmark

386   configuration.

387   For investigating trends in anchor size evolution, we first computed all possible pairwise

388   Euclidean distances between the raw landmarks in each sample. Each dorsal and ventral anchor

389   has 11 landmarks, thus generating 55 possible pairwise Euclidean distances which we used as

390   size variables. When the loadings and variables of the first principal component (PC1) have the

391   same sign, PC1 can be interpreted naturally as a measure of size (Jolliffe, 2002). Subsequently,

392   we performed continuous character mapping (implemented using `contMap` function in the

393   `phytools` package) of mean PC1 of the size variables of each species for ventral and dorsal

394   anchors onto the phylogeny of 13 *Ligophorus* species to assess clade-specific patterns of anchor

395   size evolution. The Adams-Collyer phylogenetic regression for shape response variable (Adams,

396   2014b; Collyer et al. 2015; implemented in the `geomorph` package, Version 2.1.1) was used to

397   formally test evolutionary correlation between anchor shape and two covariates: the logarithm of

398   body size and the logarithm of anchor size. The interaction between the two covariates was

399   incorporated into the phylogenetic regression model if covariate collinearity could be ruled out

400   using the Ho-Ané phylogenetic regression (Ho and Ané, 2014; implemented in the `phylolm`

401   package, Version 2.2) under a Brownian motion model for the phylogenetic covariance matrix.

402   For both regression analyses, p-values were computed via a resampling procedure with 10 000

403   iterations.

404   *Covariation of Anchor Shape and Size with Male Copulatory Organ Morphology*

405   Rohde and Hobbs (1986) hypothesized that the reproductive barrier among congeneric

406   species that share the same host can be maintained in monogenean parasites by their having

407   different copulatory organ morphology when attachment organs are similar (thus occupying

408   similar microhabitats); conversely, when parasites have dissimilar attachment organs (thus

409   occupying different microhabitats), the morphology of their copulatory organs would not show

410   important differences, since the lack of proximity puts less evolutionary pressure on the parasites

411   to evolve morphologically different copulatory organ. Qualitative evidence with limited number

412   of congeneric species (Lambert and Maillard, 1975; Roubal, 1981; Rohde et al., 1994) supported

413   the hypothesis's feasibility, as well as later studies with more species (Šimková and Morand,

414   2008, 2015). Quantitative evaluations using larger species assemblage that relied on traditional

415   morphometric data are available, but the interpretation of their results in support of the hypothesis

416   was obscured by either the problem of using inflated degrees of freedom in regression analysis

417   (e.g. Šimková et al., 2002) or failure to control for the effect of phylogeny (e.g. Jarkovský et al.,

418   2004). With the development of new tools for geometric morphometric and phylogenetic

419   comparative methods, we are in a position to retest the Rohde-Hobbs hypothesis. To this end, we

420   compared the size of the male copulatory organ (mean tube length data from Soo and Lim, 2012,

421   2015; Soo et al., 2015) and three of its selected morphological characters (Table 2: position of

422   copulatory organ entrance at the main lobe of accesory piece; accesory piece of male copulatory

423   complex; shape of accesory piece of male copulatory complex) against anchor shape and size

424   variation. Ancestral node positions were estimated as before using the `fastAnc` function in the

425   `phytools` package.

Characters	Character States	Set A		Set B
		Included in study	Index	Included in study
Male copulatory organ:				
Position of copulatory organ entrance at the main lobe of accessory piece	(0) proximal; (1) distal; (2) medial	√	1	√
Accessory piece of male copulatory complex	(0) consists of two lobes (main and secondary lobes or proximal and distal ones); (1) consists of one lobe	√	2	√
Shape of accessory piece of male copulatory complex	(0) beak or hook-shaped; (1) claw-shaped pincer-like; (2) cross-shaped; (3) funnel-shaped; (4) open, grooved tube (rod-like)	√	3	√
Female reproductive system				
Vaginal canal sclerotization	(0) present; (1) absent	√	4	√
Distal end of sclerotized vagina	(0) funnel-shaped thin-walled; (1) funnel-shaped thick-walled; (2) scyphoid narrow; (3) scyphoid broad; (4) not observed	√	5	√
Bars				
Relative size of ventral and dorsal bar	(0) subequal; (1) dorsal bar longer than ventral one; (2) ventral bar longer than dorsal one; (3) not applicable	√	6	√
Anchors				
Ratio of shaft to point of ventral anchor	(0) less than 1.4; (1) 1.4–2.6; (2) greater than 2.6	X	-	√
Ratio of shaft to point of dorsal anchor	(0) less than 1.4; (1) 1.4–2.6; (2) greater than 2.6	X	-	√
Length of ventral anchor point	(0) 7–12 μm; (1) less than 7 μm	X	-	√

Characters	Character States	Set A		Set B
		Included in study	Index	Included in study
Length of dorsal anchor point	(0) greater than 11 μm; (1) 5–11 μm; (2) less than 5 μm	X	-	√
Relation of outer root to point of ventral anchor	(0) outer root shorter than point; (1) outer root subequal or longer than point	X	-	√
Relation of outer root to point of dorsal anchor	(0) outer root shorter than point; (1) outer root subequal with point; (2) outer root longer than point	X	-	√
New characters				
Shape of ventral anchor	(0) shaft scimitar-shaped, root U-shaped (1) shaft scimitar-shaped, root V-shaped; (2) shaft sickle-shaped, root U-shaped; (3) shaft sickle-shaped, root V-shaped	√	7	X
Shape of dorsal anchor	(0) shaft scimitar-shaped, asymmetric inner and outer roots; (1) shaft sickle-shaped, symmetric inner and outer roots; (2) shaft sickle-shaped, asymmetric inner and outer roots	√	8	X

Ventral anchor: Length from L1 to L3	(0) 15μm or less; (1) greater than 15μm	√	9	X
Dorsal anchor: Length from L1 to L3	(0) 15μm or less; (1) greater than 15μm	√	10	X
Ventral anchor: Length from L1 to L5	(0) Less than 15μm; (1) 15μm - 25μm; (2) greater than 25μm	√	11	X
Dorsal anchor: Length from L1 to L5	(0) 15μm - 25μm; (1) greater than 25μm	√	12	X

426 TABLE 2.

427   *Morphological Integration Analysis*

428   The roots of the anchor are bases for muscle attachment. Biomechanically, force exerted

429   through the muscles and transmitted to the point compartment controls the anchor's grip strength

430   on the gills. Because of this, we may expect the anchor to function as a single, fully integrated

431   module (Klingenberg, 2008) on a priori grounds. Anchor shape is strongly constrained by either

432   phylogeny or convergent evolution. If the latter's effect was weak, then suitable morphological

433   characters based on variation in anchor shape can be expected to be systematically useful.

434   To date, only few morphological integration analyses in monogeneans have been done.

435   Using published morphological drawings, Vignon et al. (2011) investigated interspecific

436   modularity of attachment organs (marginal hooks, anchors and bars) in 66 *Cichlidogyrus*

437   (Monogenea: Ancyrocephalidae) species. More recently, Rodríguez-González et al. (2015a)

438   studied intraspecific morphological integration of the root and the point compartments of

439   anchors in *Ligophorus cephali*, using the partial least squares method in the context of shape

440   analysis (Rohlf and Corti, 2000). Here, we extended their morphological integration analysis to

441   the interspecific level in *Ligophorus*. We applied the phylogeny-aware partial least squares

442   method based on the evolutionary covariance matrix (Adams and Felice, 2014) to estimate the

443   extent of morphological integration between the ventral and dorsal anchors, as well as that of the

444   root compartment (L1 to L4 and L11) and the point compartment (L5 to L10) within and between

445   the ventral and dorsal anchors.

446   *New Morphological Characters from Morphometric Variables*

447   A continuous morphometric variable can be discretized and treated as a morphological

448   character with two or more states for use in a cladistic analysis (Thiele, 1993; Rae, 1998; Wiens,

449   2001). In doing so, the taxonomist relies on experience and intuition to select promising

450   morphometric variables out of a potentially large set of candidates. Unfortunately, an objective

451   means to screen the latter is generally lacking. As a result, it is difficult to assess the level of

452   homoplasy present in the taxonomist's candidate characters. Here, we show how comparison of

453   patterns of shape change in different clades leads to the discovery of new morphometric variables

454   for morphological phylogenetic analysis in *Ligophorus*. A set of 12 morphological characters

455   defined in Sarabeev and Desdevises (2014) that are not invariant for the 13 *Ligophorus* species

456   (Table 2; see Table S4 for character state matrix) was chosen. We replaced the morphological

457   characters derived from traditional morphometric measurements of anchors with new candidates

458   derived from geometric morphometric analysis to assess their phylogenetic informativeness. To

459   this end, we compared how well-resolved the resulting maximum parsimony trees (using PAUP;

460   Swofford, 2002) were. Tree search (initial tree obtained via stepwise addition) was performed

461   using the heuristic search option. Branch-swapping was done using the tree bisection and

462   reconnection algorithm. Tree reliability was assessed using 1000 bootstrap replicates and

463   branches were collapsed if bootstrap support was below 50%.

464   RESULTS

465   *Molecular Phylogeny*

466   The GTR + G model was the best DNA substitution model that did not incorporate the

467   proportion of invariable sites. After mid-point rooting, the estimated ML tree (Fig. 3; 10000

468   bootstrap replicates) contained two major clades. One of them consisted of species infecting *M.*

469   *buchanani* (Clade I), and the other consisted of species infecting *Liza subviridis* (Clade II).

470   Bootstrap support was high for most internal nodes, except the most recent common ancestor

471   node of *L. parvicopulatrix-L. bantingensis*, and *L. grandis-L. fenestrum* (between 50-60%).

472   FIGURE 3.
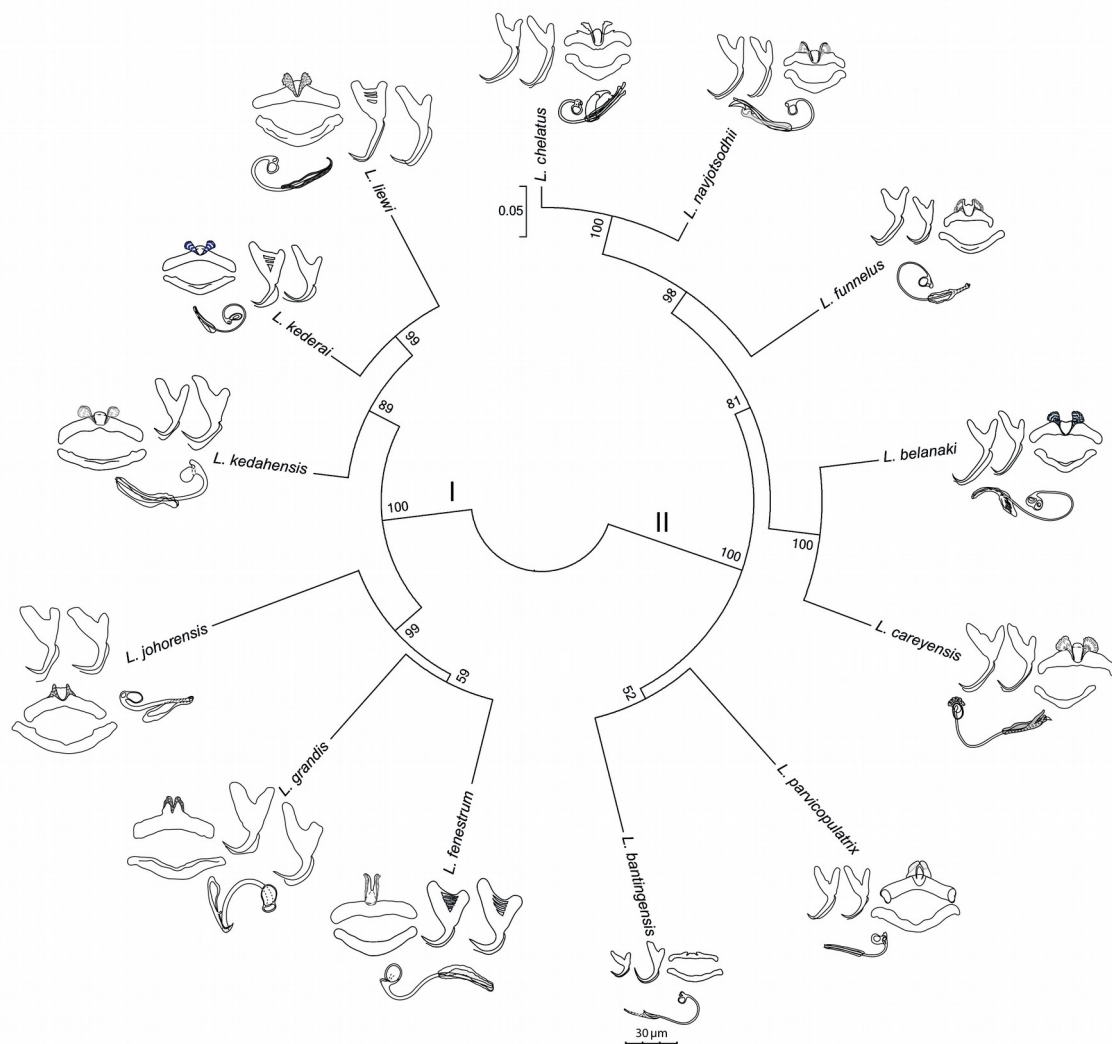
473   *Morphometry Summary Statistics*

474   Table S5 gives summary statistics of anchor size, anchor shape, body size and male

475   copulatory organ size for the 13 *Ligophorus* species.

476   *Anchor Shape and Phylogeny Correlation*

477   Scatter plots of GPA landmark configuration of all specimens for the ventral and dorsal

478   anchors are given in Fig. 4 (see Fig. S4 to Fig. S16 for species-specific alignments). Figure 5

479   shows the PCA plots of PC2 against PC1, and PC3 against PC1 for shape variables of ventral and

480   dorsal anchors (See Fig. S17 for a three-dimensional PCA plot). The first three PC accounted for

481   84% and 79% of total shape variation in the ventral and dorsal anchors, respectively. To interpret

482   these three PCs, we simultaneously compared the scatter plots of the GPA landmark

483   configurations with the heat map of shape variable loadings (Fig. S18 and S19). Anchors with a

484   sickle-shaped shaft had large positive values of PC1 (e.g. ventral anchors of *L. fenestrum, L.*

485   *grandis, L. kedahensis, L. johorensis*), while those with a scimitar-shaped shaft (e.g. ventral

486   anchors of *L. chelatus, L. belanaki, L. navjotsodhii*) had large negative values in ventral anchors.

487   For ventral anchors, large positive PC2 values were associated with V-shaped root grooves (e.g.

488   *L. bantingensis*). In contrast, the U-shaped root groove (e.g. *L. liewi, L. kederai*) was associated

489   with negative PC2 values. For dorsal anchors, PC2 was positive and large for highly symmetric

490   inner and outer roots (e.g. *L. parvicopulatrix*) and vice versa (*L. liewi, L. bantingensis, L.*

491   *grandis*). PC3 did not admit a simple geometrical interpretation.

492   The result of Adams's K_{mult} test supported the presence of significant phylogenetic signal

493   in anchor shape (K = 0.948; p-value = 0.0003). Graphically, this is reflected in the PCA plots

494   where both clades show divergent evolutionary trajectories in phylomorphospace (Fig. 5).

495   FIGURE 4.

a)

b)

Species

● *L. bantingensis*	● *L. fenestrum*	● *L. kedahensis*	● *L. parvicopulatrix*
● *L. belanaki*	● *L. funnelus*	● *L. kederai*	
● *L. careyensis*	● *L. grandis*	● *L. liewi*	
● *L. chelatus*	● *L. johorensis*	● *L. navjotsodhii*	

496   FIGURE 5.
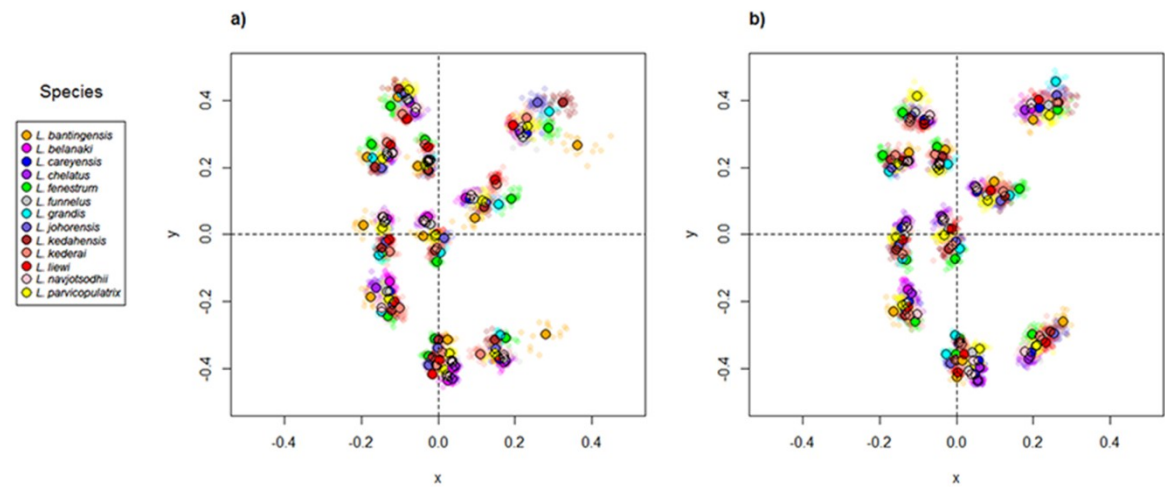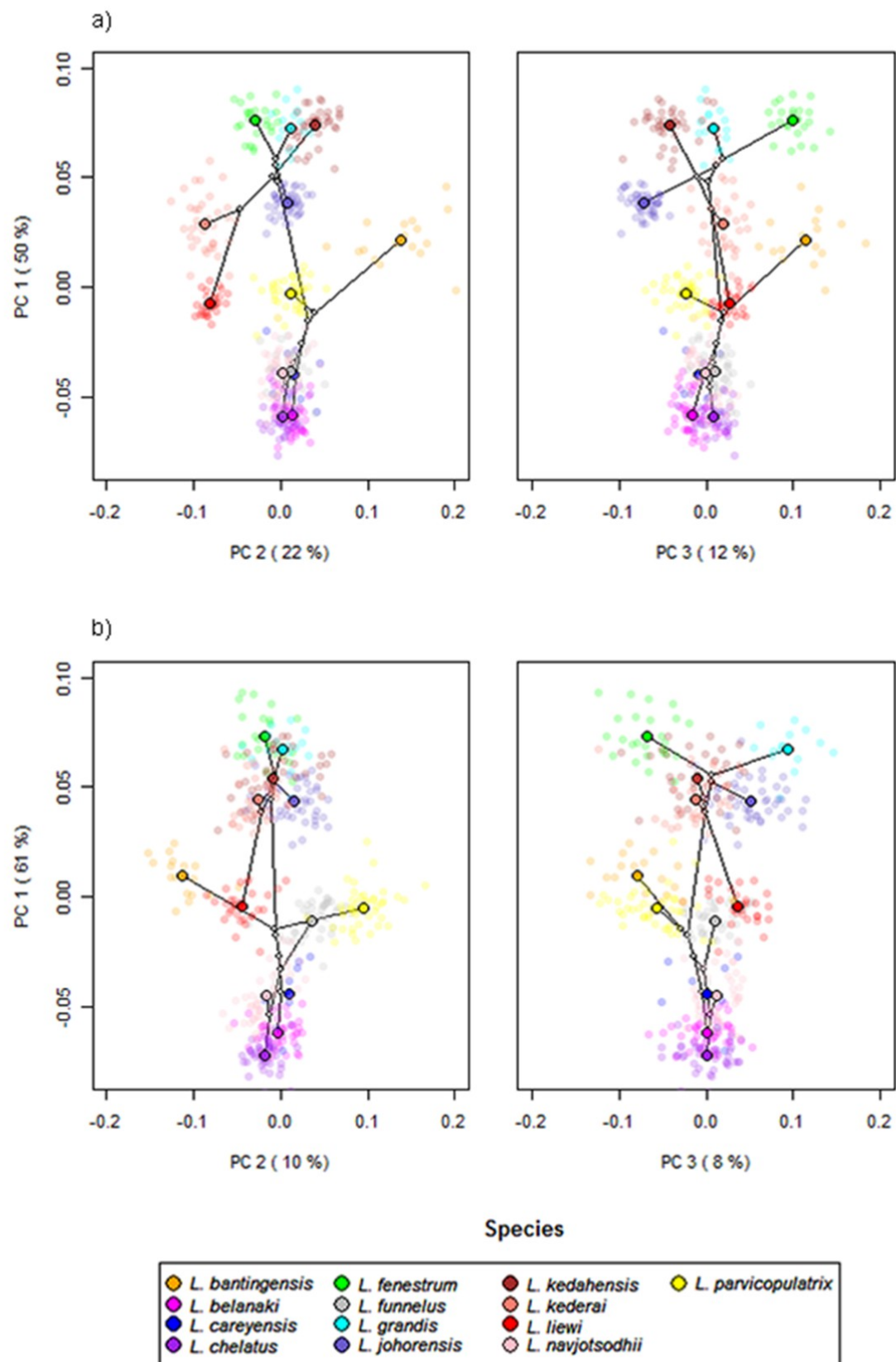
497   *Cluster Analysis of Geometric Morphometric Data*

498   The cluster heat map (Fig. 6) shows that variation in anchor shape alone allows the

499   samples to be clustered unambiguously into 12 clusters corresponding to 12 of the *Ligophorus*

500   species, confirming that between species variation is much larger than within species variation.

501   On the other hand, with only eight specimens used, the clustering outcome was ambiguous for *L.*

502   *careyensis,* whose samples were mainly clustered with *L. belanaki*.

503   FIGURE 6.
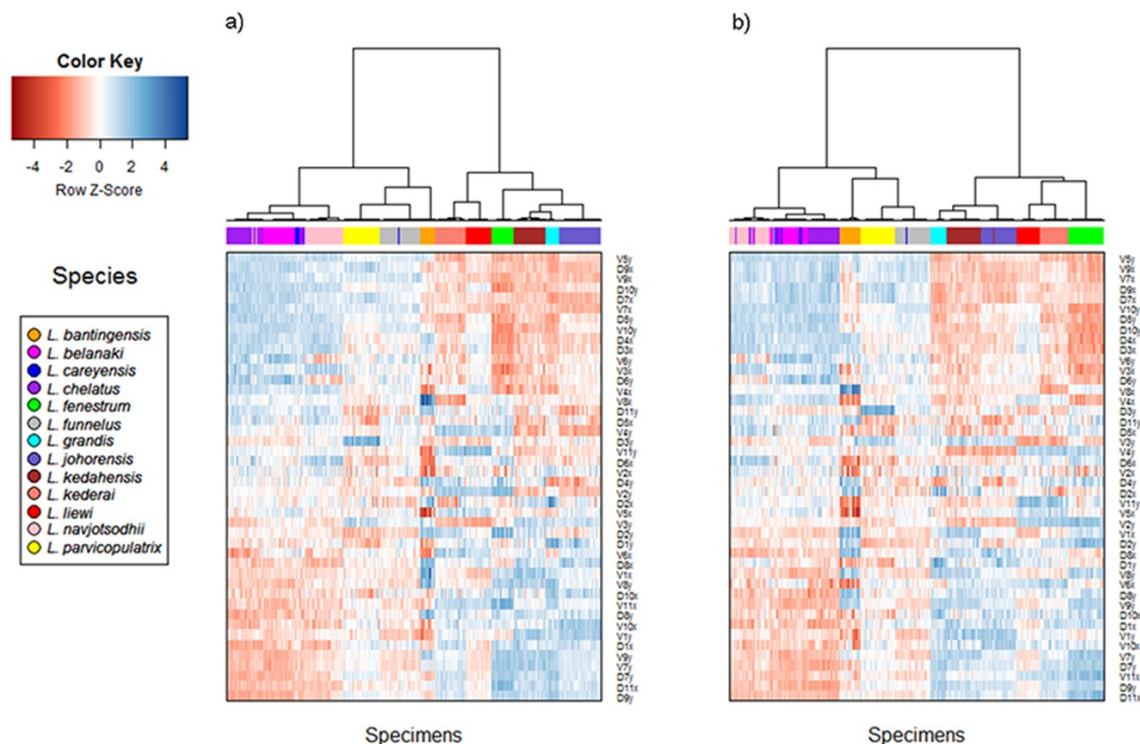
504   Consistent with the detection of significant phylogenetic signal in anchor shape,

505   hierarchical clustering revealed two major clades whose members were exactly the same as those

506   of Clade I and Clade II. The quality of clustering using specimens that passed quality control was

507   improved especially for species with anchors that have very similar shapes such as *L.*

508   *navjotsodhii* and *L. chelatus* (Misclassification error of 2.5% with filtering (Table S6); 3.8% with

509   no filtering (Table S7)).

510   For each shape variable, we labelled the samples according to their membership in Clade I

511   or Clade II, and then ranked the shape variables in descending order using the two-sample t-

512   statistic to reveal inverted block structures at the top and bottom of the heat map. The shape

513   variables that make up the top block come from the x-coordinates of LM2, LM4, LM7, LM9, and

514   y-coordinates of LM5, LM6, LM10, their values being relatively positive in species belonging to

515   Clade II compared to those in Clade I. The bottom block consists of shape variables from the x-

516   coordinates of LM1, LM6, LM10, LM11 and y-coordinates of LM1, LM7, LM8, LM9. These

517   values were relatively negative in species belonging to Clade II compared to those in Clade I.

518   Collectively, these variables suggest that the mean shape of the anchor shaft in Clade II was more

519   elongated and scimitar-like (i.e. LM5, LM6, LM10 and LM7, LM8, LM9 are relatively farther

520   from each other) while that in Clade I was more robust and sickle-like (i.e. LM5, LM6, LM10

521   and LM7, LM8, LM9 are relatively closer to each other).
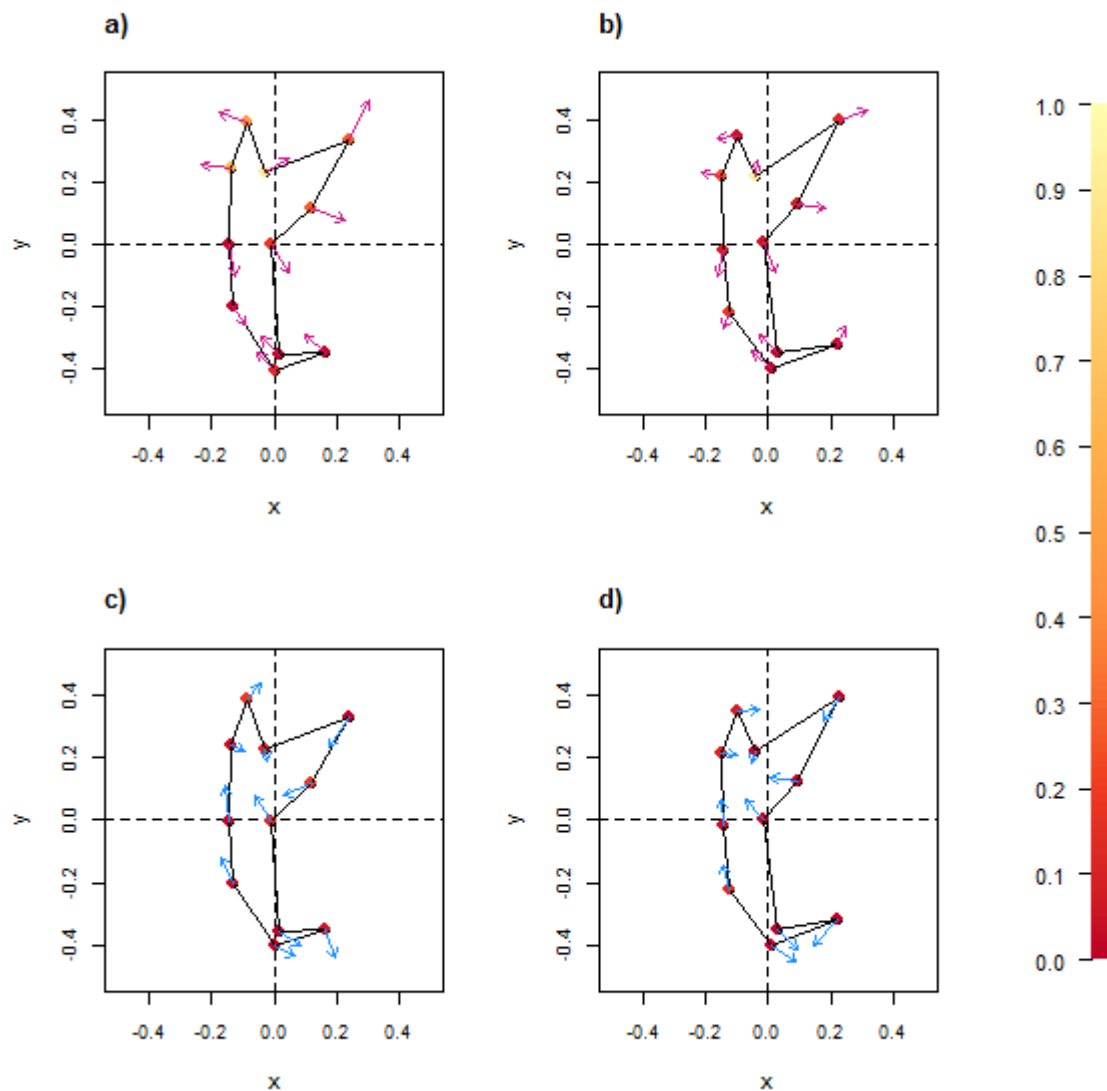
FIGURE 7.

Anchor Shape and Size Evolution

The wireframe-lollipop graphs (Fig. 7) show patterns of shape changes in the ventral and dorsal anchors of both clades that are consistent with those inferred from the cluster heat map and PCA. The circular plots (Fig. S20 and S21) provide more details at the level of individual landmarks. The explicit visualization of the direction and magnitude of GPA-landmark coordinate deviation relative to the ancestral form provides insights into selection of new morphometric variables suitable as morphological characters. Specifically, for two landmarks, if their mean directional change is divergent in one clade but convergent in another, then the interlandmark

531   distance is expected to be of value for discriminating the two clades. To be easy to measure, the

532   landmarks should be of Type I. Thus, the distance from LM1 to LM3 and from LM1 to LM5

533   were found to be good candidates. We found the common practice of using the inner root length

534   (IL) and the outer root length (OL) (distance from LM1 to LM7 and LM3 to LM7, respectively)

535   to be suboptimal since both LM3 and LM7 had almost parallel directional changes (Figs. 7a, 7c,

536   7d), whereas mean directional change in LM1 and LM7 did not show any clear patterns of

537   divergence in one clade and convergence in another (Fig. 7) to be able to show large variation

538   between Clade I and Clade II. Figure 8 (see also Fig. S22 and Fig. S23) shows that it is possible

539   to define cut-offs for the LM1-LM3 (15μm) and LM1-LM5 (25μm) distances that result in

540   discrimination of Clade I from Clade II, but no reasonable cut-offs for IL and OL lead to similar

541   results.
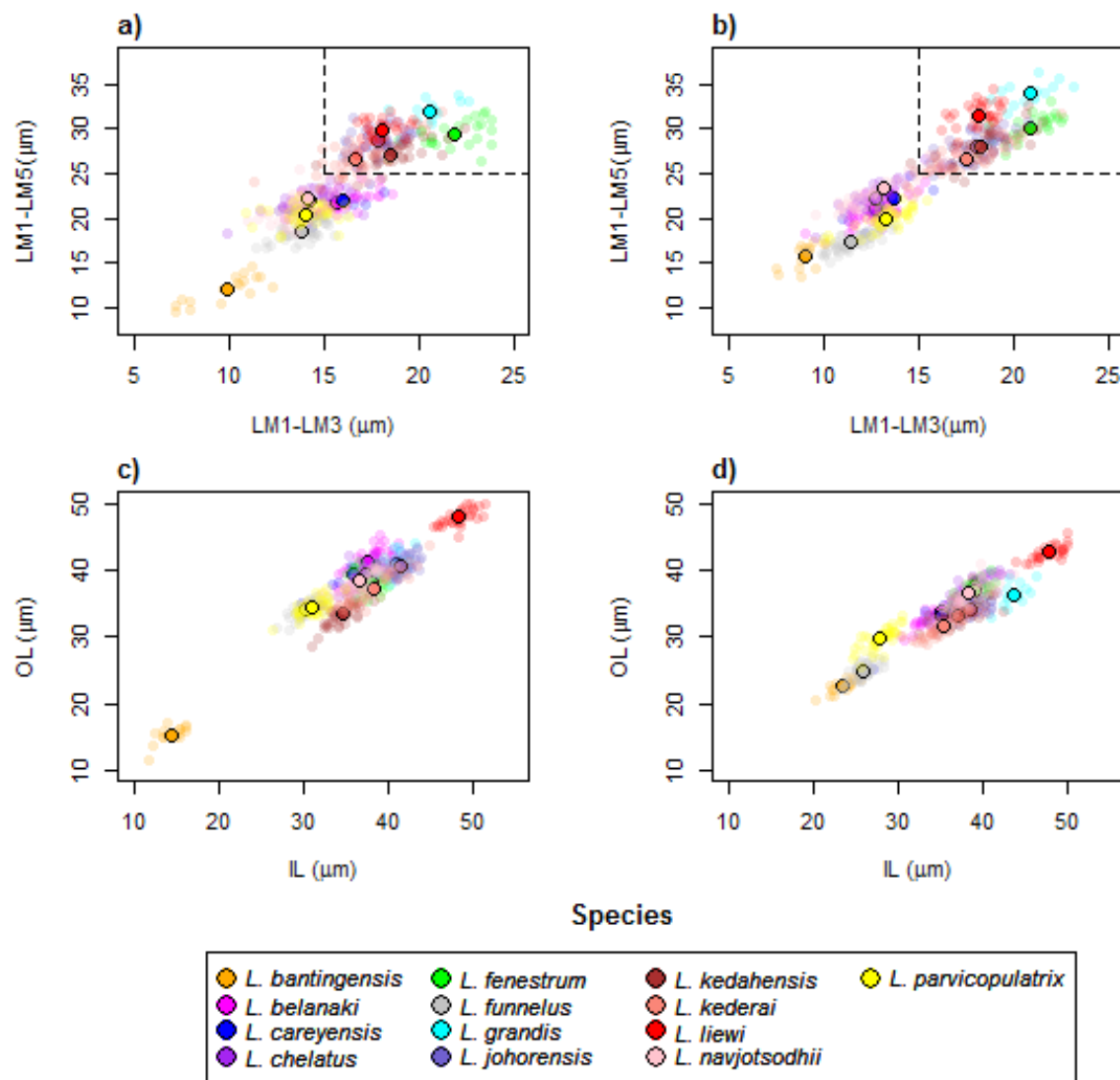
FIGURE 8.

The average median body size of species in Clade I was significantly larger compared to

Clade II (3.2 times; 95% confidence interval body size ratio = [1.5, 7]). However, larger body

size was not correlated with larger ventral or dorsal anchor size, after controlling for the effect of

phylogeny (Ho-Ané phylogenetic regression p-values > 0.2). Consequently, both of them could

be treated as independent covariates. The species in Clade I generally had larger anchors with

sickle-shaped shaft (Fig. 9; ventral anchor mean = 170μm, standard deviation (SD) = 24 μm;

dorsal anchor mean size = 165 μm, SD = 16 μm), whereas those in Clade II had smaller anchors

550   (ventral anchor mean size = 140 μm, SD = 35 μm; dorsal anchor mean size = 133 μm, SD = 24

551   μm) with scimitar-shaped shaft. Size decrease was most striking in *L. bantingensis*, being 2.7 SD

552   and 1.8 SD below the mean of all species for the ventral and dorsal anchors, respectively.

553   Conversely, size increase was most prominent in *L. liewi*, with 1.7 SD above the mean of all

554   species for both ventral and dorsal anchors. Nonetheless, the within clade trajectory for some

555   species may sometimes show considerable variation from a clade's average trajectory. For

556   example, *L. liewi* evolved a more slender shaft for its ventral and dorsal anchors, which is closer

557   to the scimitar shape found in most species in Clade II, even though its anchor size was the

558   largest. In contrast, *L. bantingensis* evolved sickle-shaped shafts in its ventral and dorsal anchors

559   (common in Clade I species like *L. fenestrum* and *L. grandis*) even though it had the smallest

560   anchor size.
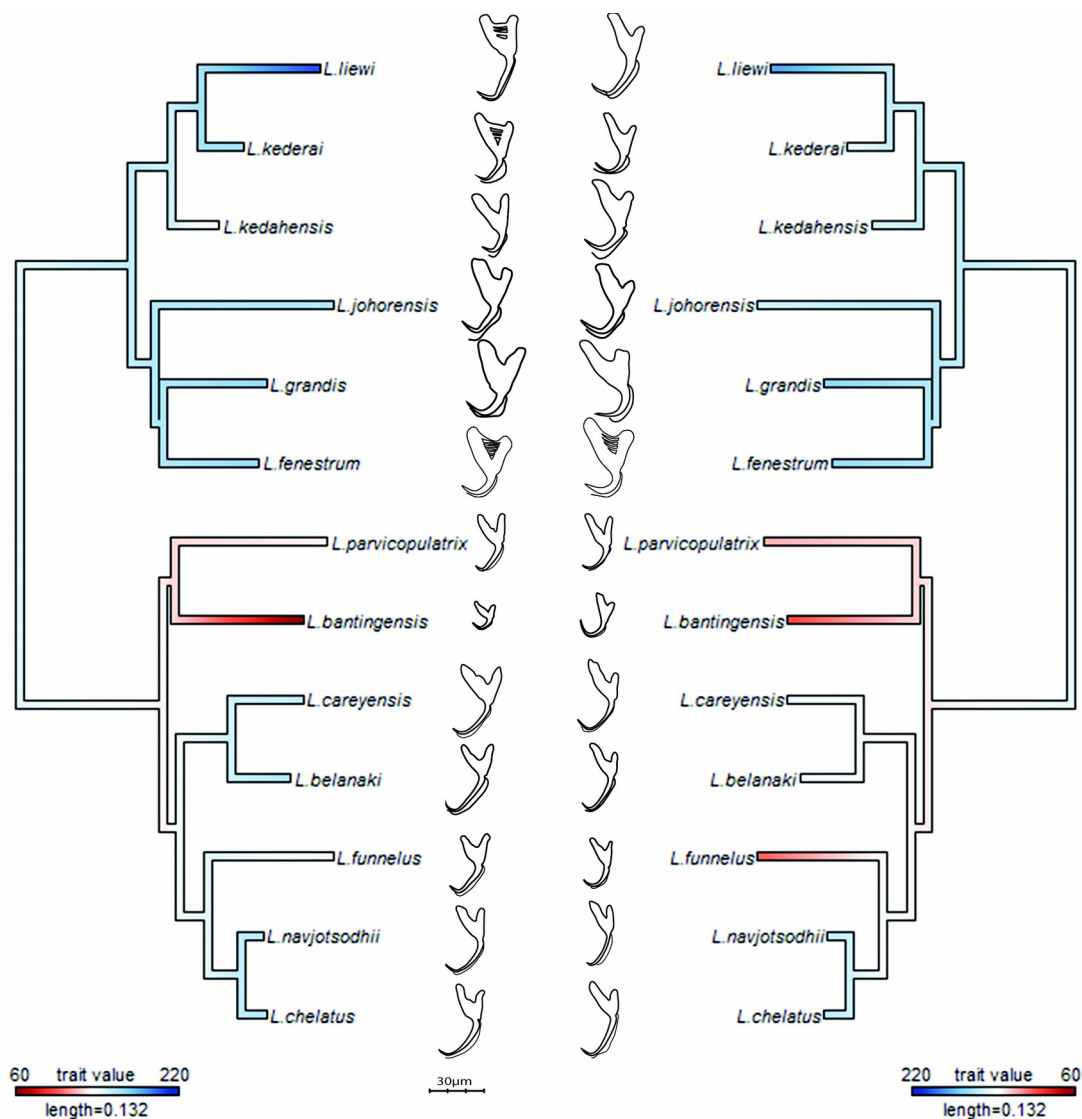
FIGURE 9.

Results from the Adams-Collyer phylogenetic regression indicated that the interaction of body size and anchor size was not statistically significant in the dorsal anchor (p-value = 0.2), but anchor size was a significant predictor of anchor shape (p-value = 0.01). For the ventral anchor, the interaction of body size and anchor size was a significant predictor of anchor shape (p-value = 0.02). Since body size and anchor shape were not significantly correlated, we may expect similar anchor shape to be found across a range of body sizes (Fig. S24).

Species

○ *L. bantingensis*	● *L. fenestrum*	● *L. kedahensis*	○ *L. parvicopulatrix*
● *L. belanaki*	● *L. funnelus*	● *L. kederai*	
● *L. careyensis*	● *L. grandis*	● *L. liewi*	
● *L. chelatus*	● *L. johorensis*	● *L. navjotsodhii*	
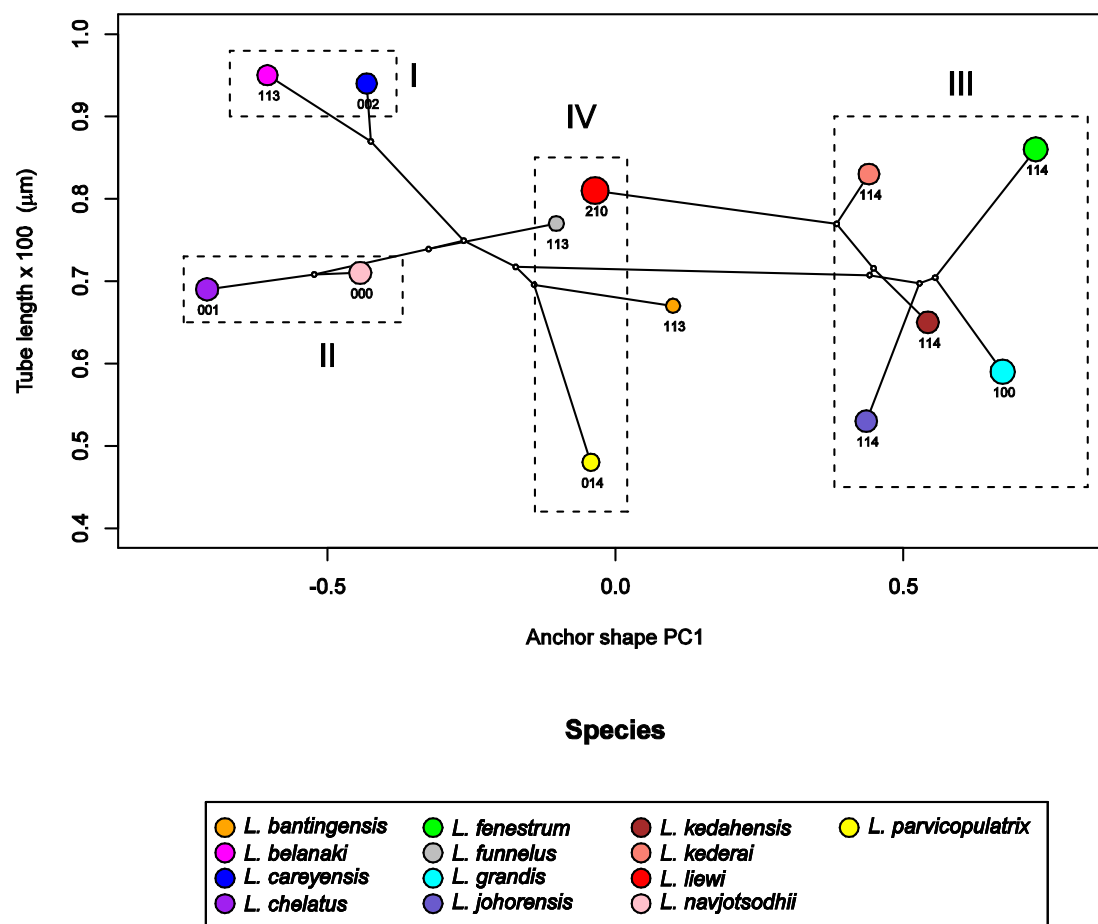
568   FIGURE 10.

569   *Patterns of Morphometric and Morphological Variation in the Male Copulatory Organ and*

570   *Anchor*

571   Where the male copulatory organ was similar in size among closely-related species with

572   similar anchor shape and size, its morphology varied (I and II in Fig.10). *Ligophorus belanaki*, *L.*

573   *careyensis*, *L. navjotsodhii* and *L. chelatus* shared a most recent common ancestor, whose

574   ancestral character states for the three male copulatory organ characters could be inferred as 113

575   on a parsimony criterion. The divergence of *L. careyensis* from *L. belanaki* did not involve major

576 changes in anchor shape, size and size of male copulatory organ, but on the latter's morphology,

577 which acquired three changes to become 002. Similarly, The most recent common ancestor of *L.*

578 *navjotsodhii* and *L. chelatus* probably evolved character states 000 or 001 from 113, and

579 divergence of these two species was associated with a change in the third character state, with

580 only relatively minor change in either anchor shape and size or copulatory organ size.

581   In contrast, where the male copulatory organ was similar in morphology among closely-

582 related species with similar anchor shape and size, its size varied (III in Fig. 10). *Ligophorus*

583 *kederai*, *L. grandis*, *L. kedahensis* and *L. johorensis* have similar anchor shape and the same

584 character states 114 for the morphology of their male copulatory organ. Consistent with

585 prediction from the Rohde-Hobbs hypothesis, substantial variation in the size of their male

586 copulatory organ was observed. It is possible for size and morphological variation to co-occur in

587 the male copulatory organ, as shown in the divergence of *L. grandis* and *L. fenestrum* from their

588 common ancestor. Finally, species with similar anchor shape (IV in Fig. 10) showed large

589 variation in both their male copulatory organ size and morphology.

590 *Morphological Integration*

591   The shapes of both ventral and dorsal anchors were strongly and significantly correlated

592 (evolutionary correlation = 0.84, Adams-Felice test p-value = 0.003). Additionally, there was

593 tight integration between the root and point compartments of the ventral (evolutionary correlation

594 = 0.85, Adams-Felice test p-value = 0.004) and dorsal anchors (evolutionary correlation = 0.86,

595 Adams-Felice test p-value = 0.001). Thus, the entire anchor can be considered as a single, fully

596 integrated module. Across the ventral and dorsal anchors, integration of the point compartments

597 was strong (evolutionary correlation = 0.92, Adams-Felice test p-value = 0.0001) but that of the

598 root compartments was weaker (evolutionary correlation = 0.79, Adams-Felice test p-value =

599   0.03). Figure S25 provides a graphical summary of the results of the morphological integration

600   analysis.

Phylogenetically Informative Morphometric Variables

602   For the current 13 *Ligophorus* species, the maximum parsimony tree estimated using the

603   set of morphological characters containing discretized LM1-LM3 and LM1-LM5 distances and

604   anchor shape was better resolved (Fig. 11) . Clade I and Clade II were clearly identified, and the

605   partially resolved relationships within each clade were also congruent with those of the molecular

606   phylogeny's. In contrast, using morphological characters of the anchors derived from traditional

607   morphometrics as in Sarabeev and Desdevises (2014) produced a maximum parsimony tree that

608   was mostly reticulate and unable to distinguish Clade I and Clade II.
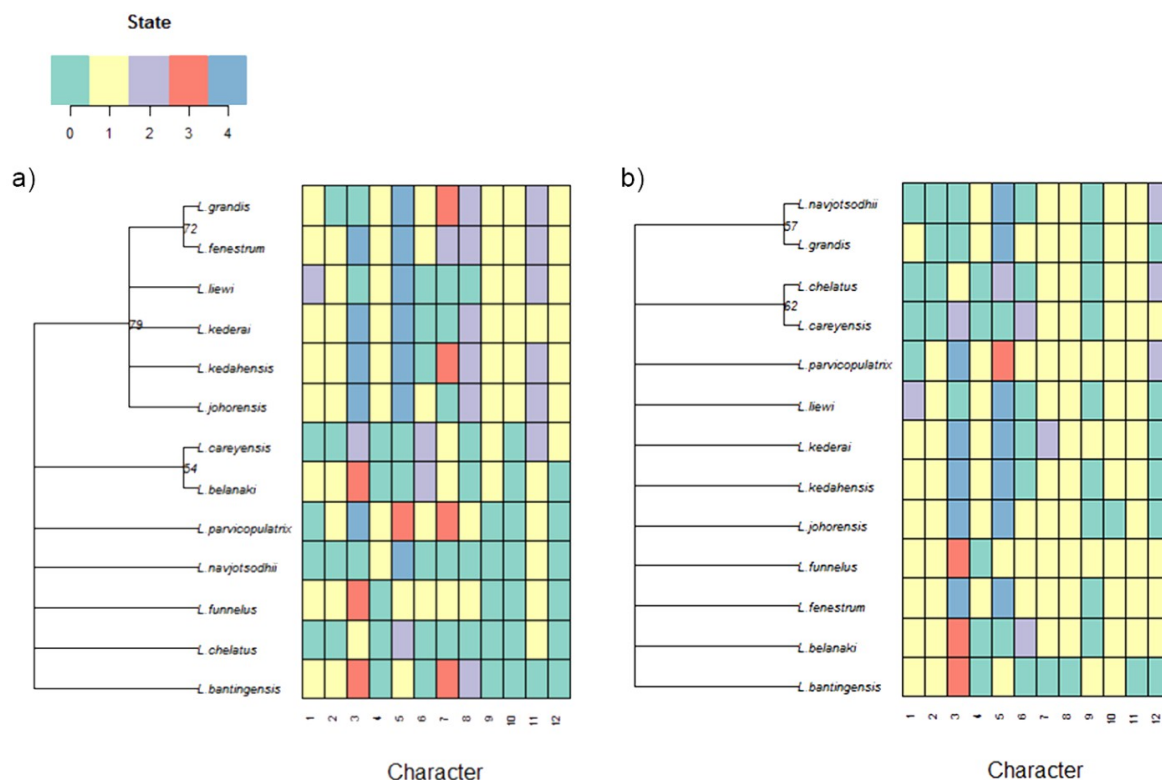
609   FIGURE 11.

610   DISCUSSION

611   *Data Quality Control*

612   We are not aware of any geometric morphometric analyses of anchors in monogeneans

613   that currently implement specimen quality control. Specimen quality introduces an important

614   source of non-biological variation into observed anchor shape variation, the impact of which

615   depends on whether the data would be analyzed at the intra or interspecific level. Thus, while the

616   inclusion of specimens that failed quality control into hierarchical clustering did not

617   fundamentally change species discrimination outcome in this study, it is important to control for

618   this confounder where intraspecific variation can be expected to impact conclusions of an

619   analysis, for example, when investigating mean directional change in landmarks of anchors (Fig.

620   7), or testing for association between intraspecific anchor shape variation and evolutionary

621   potential of a species (Rodríguez-González et al., 2015a) . In the current study, we observed up to

622   50% loss of specimens (*L. fenestrum*) due to low quality score. Assuming this value

623   optimistically as an upper bound, then at least 40 specimens per species would have to be

624   obtained in order to anticipate 20 or more specimens passing quality control. An ideal case like

625   this may not always be possible, since sampling trips do not always yield sufficient study

626   material.

627   The assumption of symmetry in the left and right side of the ventral and dorsal anchors

628   used in the quality control procedure has a caveat that should be noted. Poor quality specimens

629   that arise as a consequence of incongruent image and object planes are confounded with

630   specimens that show fluctuating asymmetry. If fluctuating asymmetry (Graham et al., 2010) is

631   common, then a large proportion of specimens would have been discarded using the quality

632   control procedure, but this is not the case in the present study, where about 82% (437/530) of all

633   specimens were retained. Careful observations over multiple well-prepared mounts should help

634 researchers decide the appropriateness of implementing the quality control step for specimens

635 from a particular monogenean genus.

636   Variation in quality scores can be attributed to several sources, such as the method of slide

637 preparation, the quality of camera lens and software used for capturing images, and the skill and

638 experience of the data gatherer. In this study, a single data gatherer (O.Y.M. Soo) prepared and

639 acquired the landmark data, using the same compound microscope and computer. Because of this,

640 we expect other factors to explain the poor quality scores. Interestingly, we note that species that

641 had larger proportion of specimens failing quality control tend to have body and/or anchor size

642 that were relatively large or small. In the case of *L. grandis* ($\log_{10}$ median body size 2.1 SD larger

643 from total mean; dorsal anchor size 1.0 SD larger than total mean), *L. fenestrum* ($\log_{10}$ median

644 body size 1.6 SD larger than total mean; dorsal anchor size 0.9 SD larger than total mean), and *L.*

645 *bantingensis* ($\log_{10}$ median body size 0.9 SD smaller than total mean; ventral anchor size 2.7 SD

646 smaller than total mean), we observed about 30%, 50% and 45% of the specimens failing

647 quality control (Q-score < 10; Fig. S2), respectively. A possible explanation may be that the

648 robust anchors of *L. fenestrum* and *L. grandis* have uneven thickness at the root and point

649 regions, which makes them difficult to evenly flatten on slides. The large body bulk may also

650 further hinder effective flattening. Monogenean anchor thickness is not usually measured but may

651 be indirectly inferred through 3D-modelling (Teo et al., 2010; Teo et al., 2013). Since size and

652 physical inertia are positvely correlated, the small body and anchor size of *L. bantingensis* make

653 specimen orientation on the slide sensitive to variation in force applied during slide flattening.

654 *Phenotypic Plasticity in Anchor Shape*

655   Different species were found to have varying levels of intraspecific phenotypic plasticity

656   in this study. While within species shape variation in both ventral and dorsal anchors was large in

657   some species (*L. kedahensis*, *L. parvicopulatrix*), it was limited in others (*L. grandis*, *L. liewi*).

658   Interestingly, the generalist *L. bantingensis*, which has been reported to be found in two small

659   fish hosts (Kritsky et al., 2013): *Liza abu* (body length range: 12-15.5 cm) and *Liza klunzingeri*

660   (body length range: 14-18cm), had the largest intraspecific shape variation in its ventral anchor,

661   particularly in its root compartment (PC2). Phenotypic plasticity within species likely promotes

662   divergence by increasing the adaptability to different gill microhabitats (Rohde and Watson,

663   1985; Poisot and Desdevises, 2010; Pfennig et al., 2010; Rodríguez-González et al., 2015a), and

664   is generally considered to be important for generalist species (van Valen, 1965; Kaci-Chaouch et

665   al., 2008; Šimková et al., 2013).

666   *Integrative Geometric Morphometric Analysis Supports the Rohde-Hobbs Hypothesis*

667   Evidence for supporting the Rohde-Hobbs hypothesis has traditionally come from

668   integrating spatial distribution data of monogeneans on gill microhabitats (e.g. Rohde, 1977;

669   Ramasamy et al., 1985; Koskivaara et al., 1992) with morphological data of the monogenean

670   species (e.g. Fig. 6.3 in Šimková and Rohde, 2013). These efforts were very laborious, but

671   crucially established anchor shape-microhabitat association. Benefitting from such insights, our

672   current integrative geometric morphometric analysis was able to reveal patterns consistent with

673   the hypothesis's predictions on how male copulatory organ size and morphology vary with

674   respect to anchor shape (Fig. 10), despite the absence of spatial distribution data for the 13

675   *Ligophorus* species across gill microhabitats.

676   *Morphological Integration, Phylogenetic Signal and Morphological Phylogenetics*

677   In their intraspecific study of morphological integration between the root and point

678   compartments in *L. cephali*, Rodríguez-González et al. (2015a) reported only modest degree of

679   integration in the same anchor, but stronger compartmental integration between the ventral and

680   dorsal anchors. On the other hand, using interspecific data, we demonstrated a much stronger

681   degree of integration between the root and the point compartments within anchors, and showed

682   relatively weaker integration of the root compartments between ventral and dorsal anchors.

683   Intuitively, intraspecific compartmental integration within the same anchor is expected to be high,

684   so a possible explanation for the discrepancy may be the lack of a quality control procedure for

685   filtering poor quality slides. Without the latter, it seems difficult to rule out the possibility that the

686   observed intraspecific anchor shape variation in *L. cephali* may contain non-trivial amount of

687   artifactual noise.

688   Generally, a certain degree of homoplasy may be expected in the morphology of

689   attachment organs in parasites, on grounds that functional requirements for attaching to the host

690   and adapting to within-host microhabitats would override shape constraints imposed by

691   phylogeny (Morand et al., 2002). Such form of adaptive evolution can cause K_{mult} to become less

692   than 1 (Blomberg et al. 2003). In the present *Ligophorus* phylogeny, the K_{mult} value of 0.948 is

693   significantly larger than 0 (p-value 0.0003), but slightly biased downwards from the expected

694   value under Brownian motion evolution for anchor shape. The reason seems to be that, although

695   anchor shape is more or less lineage-dependent in the present set of *Ligophorus* species, three

696   species: *L. liewi* (Clade I), *L. funnelus* (Clade II) and *L. parvicopulatrix* (Clade II), have similar

697   shaft shape (Fig. 9), despite being from different lineages, thus lowering K_{mult}. To put the

698   magnitude of K_{mult} in perspective, its univariate version - Blomberg's K statistic, has been found

699   to be generally less than 1 for numerous primate traits, exceeding 1 only for brain size (Kamilar

700   and Cooper, 2013).

701   The phylogeny (Bakke et al., 2002; Vanhove et al., 2015), immunophysiology (Buchmann

702   and Lindenstrøm, 2002), ecology (Šimková et al., 2006), and behaviour of the fish hosts (Cable et

703   al., 2002; Mendlová and Šimková, 2014) all contribute to determine patterns of infection and

704   transmission, host specificity, and subsequent mode of speciation in their monogenean parasites

705   (Littlewood et al., 1997; Cribb et al., 2002; Whittington and Kearn, 2011;Vanhove and Huyse,

706   2015). Therefore, it is not surprising that different monogenean families may show different

707   degrees of morphology-phylogeny covariation. In *Lamellodiscus* (Family: Diplectanidae), the

708   lack of cospeciation between host-parasite (Desdevises et al., 2002) suggests that adaptation to

709   host after host-switching would lead to convergent evolution in some of the morphologies (but

710   see Machkewskyi et al., 2014). Indeed, Poisot et al. (2011) found morphological features of

711   sclerotized haptor and male copulatory organs to be weakly associated with phylogeny in

712   *Lamellodiscus*. On the other hand, in *Cichlidogyrus* (Family: Ancyrocephalidae), sclerite

713   (including anchors) shape was found to contain significant phylogenetic signal (Vignon et al.,

714   2011). However, this conclusion needs to be qualified in light of the recent demonstration of a

715   host-switching event in *Cichlidogyrus* (Messu Mandeng et al., 2015), which was missed in

716   Vignon et al. (2011) because the host range (at the familial level of the fish hosts) of

717   *Cichlidoygrus* was not taken into consideration. For *Ligophorus*, the significant phylogenetic

718   signal found in the anchors does not appear to need similar qualification, since its host range is

719   currently known to be restricted to mullets. In an examination of over 1000 fish from 10 fish

720   families in the Black Sea, Öztürk and Özer (2014) observed that *Ligophorus* was restricted to

721   mullets (*Mugil cephalus* and *Liza aurata*), with almost 100% prevalence in the hosts.

722   Nevertheless, since it has been reported that a combination of host-switching (within fish host

723   family) and intra-host speciation events probably generated the present diversity of *Ligophorus*

724   species in the Mediterranean basin (Blasco-Costa et al., 2012), a more definitive conclusion

725   regarding phylogenetic signal in the anchors requires additional tests using samples of

726   *Ligophorus* species from that region.

727   The anchor morphology-phylogeny correlation shown for *Ligophorus* in the present study

728   suggests new morphological variables from the anchors that are potentially useful in

729   morphometric analysis and also morphological phylogenetics. In particular, we suggest more

730   active exploration of the newly proposed morphometric variables: the distance between the inner

731   root point and the outer root point (LM1 – LM3), and the distance between the inner root point

732   and the dent point (LM1 – LM5), as alternatives to existing usage of the inner root length (IL)

733   and the outer root length (OL) in traditional morphometric analysis. The discretization of the two

734   proposed morphometric variables: anchor shaft shape and anchor shaft shape, can also be further

735   considered in future morphological phylogenetic analysis.

736   *Anchor Shape and Size Correlation with Host and Ecological Factors*

737   In the present study, the modest levels of anchor shape-size covariation revealed through

738   the Adams-Collyer phylogenetic regression analysis for the 13 *Ligophorus* species suggest that,

739   apart from the effect of shared ancestry, anchor shape-size covariation is likely non-trivially

740   constrained by additional factors, one of which could be their biomechanical compatibility.

741   Another factor is host size and ecology. On average, the larger *Moolgarda buchanani* (body

742   length range 35-48cm) harbored larger *Ligophorus* species, whereas the smaller *Liza subviridis*

743   (body length range 25-30cm) harbored smaller *Ligophorus* species.

744   The current analysis showed that *L. bantingensis* evolved anchors of a smaller size but

745   retained the sickle-shape shaft common in Clade I, which is associated with larger anchor size.

746   The observed small anchor size is consistent with the hypothesis that small or medium-sized

747   attachment organs are generally associated with a generalist lifestyle, as these sizes expand the

748   host range of monogeneans to small or medium-sized hosts, which are generally more diversified

749   than larger hosts (Morand et al., 2002).

750   In the present study, open seas (Langkawi Island) yielded only *M. buchanani* samples

751   whereas sheltered marine environment yielded both *M. buchanani* and *Liza subviridis* samples.

752   This suggests that perhaps the larger and more robust anchors in *Ligophorus* species infecting

753   *M.buchanani* may be a consequence of the hosts' adaptation to rough open seas, where strong

754   water currents are expected. In such conditions, burst swimming is an important locomotory

755   strategy for the fish host, not only to negotiate strong currents, but also to chase swift preys and

756   avoid strong predators (Koehn and Crook, 2013). Indeed, for skin-parasitic fish monogeneans,

757   their attachment appendages must be able to withstand dislodgement by strong water currents

758   pushing against the fish surface as the fish host performs burst swimming (Kearn, 2014).

759   Concurrently, it seems plausible that burst swimming may also, for a short time, cause strong

760   water currents to flow through the gill chamber, thus imposing a selective pressure for more

761   robust anchors in monogeneans that live on the gills.

762   The U-shaped root groove in some species infecting *M. buchanani* (e.g. *L. liewi*, *L.*

763   *kederai* and *L. fenestrum*), which could result from the accretion of sclerotic material in the space

764   between the inner and the outer root (Klaus Rohde, pers. comm., 2014), may have substantially

765   expanded the root base, providing space for connection with more muscle tissues. This would

766   likely have resulted in anchors with stronger contraction strength, necessitating the evolution of

767   the shorter but more robust sickle-shaped shaft, hence the finding of tight morphological

768   integration between the root and point compartments.

769   Interestingly, U-shaped roots and sickle-shaped shaft are also common in *Cichlidogyrus*

770   species (Vignon et al., 2011), which infect the cichlids in Africa. Ecologically, it seems unlikely

771   that such robust shapes would have evolved in freshwater environments, where cichlids are

772   mostly found. If the ancestors of cichlids and their monogenean parasites were marine in origin,

773   or host switching occurred with contact between salt-tolerant cichlids and the marine ancestor of

774   the monogenean parasite, the observed robust shapes would then be inherited, with their shapes

775   constrained by phylogeny. While some studies (Murray, 2001) suggested that the ancestors of

776   cichlids were likely marine, others were sceptical (Chakrabarty, 2004; Sparks and Smith, 2005).

777   Joint consideration of the morphology and phylogeny of monogenean fauna of cichlids and other

778   marine fishes is probably required (Pariselle et al., 2011) to assess the competing claims. For

779   example, a recent molecular phylogenetic analysis using 28S rRNA sequence (Tan, 2013; Fig.

780   S26) indicated that *Ligophorus* (marine) and *Cichlidogyrus* (mostly freshwater) species shared

781   the most recent common ancestor.

782   In three species (*L. grandis, L. funnelus* and *L. liewi*), fenestration in the anchor base

783   seems to be an invariant character state, as all examined specimens (n=22,50,32, respectively)

784   showed consistent presence of fenestration. Presently, the ecological significance of fenestrations

785   in anchors is unclear. Some progress may be possible with biomechanical studies (e.g. Wong and

786   Gorb, 2013) that compare whether fenestrated and non-fenestrated anchors differ significantly in

787   their resistance against turbulence and strong water currents. The present phylogenetic analysis

788   suggests that fenestration is not a synapomorphic character state (Fig. 3), but a clearer picture

789   requires more extensive taxa sampling.

790   *Outlook for Geometric Morphometric Analysis of Sclerotized Haptoral Structures in*
791   *Monogenean Parasites*

792   The use of less sophisticated methods could have also answered the biological problems

793   that were studied in the present work. For example, to infer the presence of phylogenetic signal in

794   attachment organs, or to investigate anchor size correlation with parasite and host phylogeny, one

795   could map qualitative shape and size categories of the organ of interest onto the molecular

796   phylogeny of the parasites, as done in Šimková et al. (2006). Validation of the Rohde-Hobbs

797   hypothesis could be done by correlating parasite abundance data in different gill microhabitats

798   with their attachment organ and male copulatory organ morphology. The lack of a unified

799   quantitative framework, however, forces the researcher to use different data types to address each

800   question. We have shown in the present work that, if geometric morphometric data is used as a

801   starting point, all the preceding questions can be simultaneously answered. In fact, the geometric

802   morphometric approach is the key that unlocks the potential of shape information in the organs of

803   interest for broader research questions, such as species and biogeographical population

804   discrimination (Vignon and Sasal, 2010), morphological integration (e.g. Vignon et al. 2011;

805   Rodríguez-González et al., 2015a), and more recently, canalization and developmental stability

806   (Llopis-Belenguer et al. 2015), all of which cannot be answered satisfactorily using traditional

807   morphometric or qualitative methods.

808   Our present study used large numbers of samples, averaging about 35 per species.

809   Compared to laborious measuring of selected lengths as done in traditional morphometrics, data

810   acquisition is far more efficient with a landmark digitization software such as TPSDIG2, which

811   simultaneously captures shape and size variation information. This improved efficiency is

812   important – by greatly reducing the tedium associated with measuring many lengths per

813   specimen, there is more incentive to sample more extensively.

814   Although the geometric morphometric approach has been strongly advocated by Vignon

815   and Sasal (2010) as an effective means to pursue systematics research in monogeneans, the

816   scientific community still lack integrative tools that would make it easy to share data and adopt a

817   common analysis pipeline to ease comparison of old and new results. Here, the `monogeneaGM`

818   R package that we have developed enables substantial number of shape and size variables from

819   large number of samples to be analyzed efficiently to answer multiple questions, ranging from

820   systematic value of the sclerotized haptoral structures to understanding patterns of phenotypic

821   and phylogenetic correlation. We hope the development of `monogeneaGM` will contribute to

822   reducing the bottleneck for large scale data analysis in the study of monogeneans. Indeed, as

823   there has been a surge in alpha taxonomy and systematic biology studies of *Ligophorus* in recent

824   years (Abdallah et al., 2009; Siquier and Ostrowski de Núñez, 2009; Blasco-Costa et al., 2012;

825   Dmitrieva et al., 2012, 2013; Soo and Lim, 2012, 2015; El Hafidi et al., 2013; Kritsky et al.,

826   2013; Sarabeev and Desdevises, 2014; Marchiori et al., 2015; Rodríguez-González et al., 2015b;

827   Soo et al., 2015), the analysis can only get more interesting as data from other species from other

828   hosts in other geographical regions are added. We expect the data analysis tools in

829   `monogeneaGM` to continue to evolve to handle complexities of data analysis when this happens.

830   The use of two-dimensional landmark data implies that the analysis of anchor size and

831   shape evolution is necessarily approximate, since some of the potential biological variation in

832   anchor morphometry may only be adequately captured in three dimensions (Galli et al., 2007).

833   Nevertheless, given the wealth of corroborative inference regarding anchor shape and size

834   evolution that have been obtained in the current study, it appears that no general loss of

835   interpretability arises from usage of two-dimensional data for geometric morphometric analysis

836   in *Ligophorus*.

837   *Future Prospects*

838   Adequate taxa coverage remains an important factor for accurate phylogenetic inference

839   (Sanderson et al., 2010). The three markers used in this study are the most common ones reported

840   for other known *Ligophorus* species in the GenBank database, hence their continued use supports

841   efforts at expanding taxa sampling of molecular sequences. Indeed, a research program in

842   *Ligophorus* systematics that expands taxa coverage of anchor geometric morphometric and

843   sequence data opens up the possibility of using parasite phylogeny and anchor morphometry to

844   test hypotheses of host genealogy and ecology (Nieberding and Olivieri, 2007) in grey mullets

845   (Teleostei: Mugilidae), a speciose fish family that is economically important (Durand et al.,

846   2012). Moreover, analysis of patterns of congruence between the phylogenies of the fish host

847   species and their *Ligophorus* parasites can provide insights into prevalence of host switching

848   (Zietara and Lumme, 2002; Vanhove and Huyse, 2015) and thence the relative importance of

849   allopatric and sympatric speciation (Huyse et al., 2003) in shaping the diversity of this genus. It is

850   also possible to expand this analysis in a biogeographic context by sampling different

851   geographical populations of a host species, since some *Ligophorus* species have been reported to

852   be useful biological markers of geographical fish host populations (El Hafidi et al., 2013). Lastly,

853   we suggest that the present methods of generating and treating geometric morphometric data

854   from the anchors, and possibly other sclerotized hard parts, can be extended to other monogenean

855   families with little difficulty.

856   CONCLUSIONS

857   The presence of significant phylogenetic signal in the anchors makes the quantitative

858   analysis of their shape and size variables useful in answering species discrimination and

859   evolutionary problems in *Ligophorus* specifically, and in other monogenean genera more

860   generally. In this study, we inferred two major host-specific clades from DNA sequence data,

861   which corroborated well with clades inferred from geometric morphometric data of anchors. We

862   further extracted size information through the first principal component of size variables based on

863   all pairwise Euclidean distances between landmarks, and showed that the *Ligophorus* species

864   infecting *Moolgarda buchanani* generally evolved larger anchors compared to those infecting

865   *Liza subviridis*. Anchor shape was correlated with anchor size after controlling for the effect of

866   phylogeny. Subsequently, through the analysis of directional change, we discovered two new

867   morphological characters based on the length between the inner root length and the outer root

868   length, and the length between the inner root point and the dent point, which proved more

869   phylogenetically informative than existing characters based on the inner length and the outer

870   length. The Rohde-Hobbs hypothesis was validated in the 13 species of *Ligophorus* considered,

871   suggesting the exploitation of different microhabitats and subsequent evolution of reproductive

872   barriers in the form of highly variable male copulatory organ size and morphology after intrahost

873   speciation. Finally, we demonstrated evidence for significant interspecific morphological

874   integration of the root and point compartments within the anchors, as well as integration of the

875   same compartment between the ventral and dorsal anchors.

876   SOFTWARE AVAILABILITY

877   The `monogeneaGM` package is available for download at https://cran.r-

878   project.org/web/packages/monogeneaGM/. Analyses in this study can be replicated using the R

879   scripts deposited in Supplemental Material C1.

880   ACKNOWLEDGMENTS

881   This work is dedicated to the memory of Lee Hong Susan Lim (1952-2014; see Gibson

882   and Ng, 2014), who conceived the present project. Susan Lim contributed actively to global

883   monogenean systematics for decades, and was instrumental at developing and transmitting this

884   art in Malaysia. Klaus Rohde read the early version of the manuscript and provided helpful

885   feedback. We thank Thian Liang Cheow for contributing R codes for data processing. Maarten

886   Vanhove helpfully pointed out some very recent studies that were useful for the Discussion

887   section. Finally, we are grateful to Jean-Lou Justine (Academic Editor), Timothée Poisot, and an

888   anonymous reviewer for their constructive comments which stimulated important improvements

889   to the present work.

890   REFERENCES

891   Abdallah V.D., de Azevedo R.K., Luque J.L. 2009. Four new species of *Ligophorus* (Monogenea:

892   Dactylogyridae) parasitic on *Mugil liza* (Actinopterygii: Mugilidae) from Guandu River,

893   southeastern Brazil. J. Parasitol. 95: 855-864.

894   Adams D.C. 2014a. A generalized K statistic for estimating phylogenetic signal from shape and

895   other high-dimensional data. Syst. Biol. 63: 685-697.

896   Adams D.C. 2014b. A method for assessing phylogenetic least squares models for shape and

897   other high-dimensional multivariate data. Evolution 68: 2675-2688.

898   Adams D.C., Felice R.N. 2014. Assessing trait covariation and morphological integration on

899   phylogenies using evolutionary covariance matrices. PLoS ONE 9(4): e94335.

900   Adams D.C., Otarola-Castillo E. 2013. geomorph: an R package for the collection and analysis

901   of geometric morphometric shape data. Methods Ecol. Evol. 4: 393-399.

902   Adams D.C., Rohlf F.J., Slice D.E. 2004. Geometric morphometrics: ten years of progress

903   following the "revolution". Ital. J. Zool. 71: 5-16.

904   Adams D.C., Rohlf F.J., Slice D.E. 2013. A field comes of age: geometric morphometrics in the

905   21st century. Hystrix 24: 7-14.

906   Adler D., Murdoch D., Nenadic O., Urbanek S., Chen M., Gebhardt A., Bolker B., Csardi G.,

907   Strzelecki A., Senger A. ~~et al.~~ 2014. rgl: 3D visualization device system (OpenGL). R package

908   version 0.95.1201. Available at http://CRAN.R-project.org/package=rgl.

909   Agostinelli C., Lund U. 2013. R package 'circular': Circular Statistics (version 0.4-7). Available

910   at:https://r-forge.r-project.org/projects/circular.

911 Arnqvist G., Mårtensson T. 1998. Measurement error in geometric morphometrics: empirical

912 strategies to assess and reduce its impact on measures of shape. Acta Zool. Acad. Sci. H. 44: 73-

913 96.

914 Bakke T.A., Harris P.D., Cable J. 2002. Host specificity dynamics: observations on gyrodactylid

915 monogeneans. Int. J. Parasitol. 32: 281-308.

916 Barão K.R., Gonçalves G.L., Mielke O.H.H., Kronforst M.R., Moreira G.R.P. 2014. Species

917 boundaries in *Philaethria* butterflies: an integrative taxonomic analysis based on genitalia

918 ultrastructure, wing geometric morphometrics, DNA sequences, and amplified fragment length

919 polymorphisms. Zool. J. Linn. Soc. 170: 690-709.

920 Batschelet E. 1981. Circular Statistics in Biology. London: Academic Press.

921 Blair D. 2006. Ribosomal DNA Variation in Parasitic Flatworms. In: Maule A.G., Marks N.J.,

922 editors. Parasitic Flatworms: Molecular Biology, Biochemistry, Immunology and Physiology.

923 Wallingford: CAB International. p. 96-123.

924 Blasco-Costa I., Miguez-Lozano R., Balbuena J.A. 2012. Molecular phylogeny of species of

925 *Ligophorus* (Monogenea: Dactylogyridae) and their affinities within the Dactylogyridae.

926 Parasitol. Int. 61: 619-627.

927 Blomberg S.P., Garland T., Ives A.R. 2003. Testing for phylogenetic signal in comparative data:

928 behavioral traits are more labile. Evolution 57: 717-745.

929 Boeger W.A., Kritsky D.C. 1997. Coevolution of the Monogenoidea (Platyhelminthes) based on a

930 revised hypothesis of parasite phylogeny. Int. J. Parasitol. 27: 1495-1511.

931 Boeger W.A., Kritsky D.C. 2001. Phylogenetic relationships of the Monogenoidea. In:

932 Littlewood D.T.J., Bray R.A. editors. Interrelationships of the Platyhelminthes. London: Taylor &

933 Francis. p. 92-102.

934 Buchmann K., Lindenstrøm T. 2002. Interactions between monogenean parasites and their fish

935 hosts. Int. J. Parasitol. 32: 309-319.

936 Cable J., Scott E.C.G., Tinsley R.C., Harris P.D. 2002. Behavior favoring transmission in the

937 viviparous monogenean *Gyrodactylus turnbulli*. J. Parasitol. 88: 183-184.

938 Chakarabarty P. 2004. Cichlid biogeography: comment and review. Fish Fish. 5: 97-119.

939 Collyer M.L., Sekora D.J., Adams D.C. 2015. A method for analysis of phenotypic change for

940 phenotypes described by high-dimensional data. Heredity 115: 357-365.

941 Conesa M.A., Mus M., Rosselló J.A. 2012. Leaf shape variation and taxonomic boundaries in

942 two sympatric rupicolous species of *Helichrysum* (Asteraceae: Gnaphalidae), assessed by linear

943 measurements and geometric morphometry. Biol. J. Linn. Soc. 106: 498-513.

944 Cribb T.H., Chisholm L.A., Bray R.A. 2002. Diversity in the Monogenea and Digenea: does

945 lifestyle matter? Int. J. Parasitol. 32: 321-328.

946 Cruz R.A.L., Pante M.J.R., Rohlf F.J. 2012. Geometric morphometric analysis of shape variation

947 in *Conus* (Gastropoda: Conidae). Zool. J. Linn. Soc. 165: 296-310.

948 De Meeus T., Michalakis Y., Renaud F. 1998. Santa Rosalia revisited: or why are there so many

949 kinds of parasites in 'The Gardern of Earthly Delights'? Parasitol. Today 14: 10-13.

950   Desdevises Y., Morand S., Jousson O., Legendre P. 2002. Coevolution between *Lamellodiscus*

951   (Monogenea; Diplectanidae) and Sparidae (Teleostei): the study of a complex host-parasite

952   system. Evolution 56: 2459-2471.

953   Dmitrieva E.V., Gerasev P.I., Gibson D.I., Pronkina N.V., Galli P. 2012. Descriptions of eight new

954   species of *Ligophorus* Euzet & Suriano, 1977 (Monogenea: Ancyrocephalidae) from Red Sea

955   mullets. Syst. Parasitol. 81: 203-237.

956   Dmitrieva E.V., Gerasev P.I., Gibson D.I. 2013. *Ligophorus abditus* n. sp. (Monogenea:

957   Ancyrocephalidae) and other species of *Ligophorus* Euzet & Suriano, 1977 infecting the flathead

958   grey mullet *Mugil cephalus* L. in the Sea of Japan and the Yellow Sea. Syst. Parasitol. 85: 117-

959   130.

960   Durand J.D., Shen K.N., Chen W.J., Jamandre B.W., Blel H., Diop K., Nirchio M., Garcia de

961   Leon F.H., Whitfield A.K., Chang C.W., Borsa P. 2012. Systematics of the grey mullets

962   (Teleostei: Mugiliformes: Mugilidae): molecular phylogenetic evidence challenges two centuries

963   of morphology-based taxonomy. Mol. Phylogenet. Evol. 64: 73-92.

964   El Hafidi F., Rkhami O.B., de Buron I., Durand J-D., Pariselle A. 2013. *Ligophorus* species

965   (Monogenea: Ancyrocephalidae) from *Mugil cephalus* (Teleostei: Mugilidae) off Morocco with

966   the description of a new species and remarks about the use of *Ligophorus* spp. as biological

967   markers of host populations. Folia Parasitol. 60: 433-440.

968   Felsenstein J. 1981. Evolutionary trees from DNA sequences: a maximum likelihood approach. J.

969   Mol. Evol. 17: 368-376.

970   Felsenstein J. 2003. Inferring Phylogenies. Sunderland, MA: Sinaeur Associates.

971 Galli P., Strona G., Villa A.M., Benzoni F., Stefani F., Doglia S.M., Kritsky D.C. 2006. Two-

972 dimensional versus three-dimensional morphometry of monogenoidean sclerites. Int. J. Parasitol.

973 37: 449-456.

974 Gibson D.I., Ng P.T.K. 2014. Lim Lee Hong, Susan (1952-2014) – monogenean systematist and

975 Commisioner 2006-2014. Bull. Zool. Nomen. 71: 217-220.

976 Gilmore S.R., Cone D.K., Lowe G., King S.K., Jones S.R.M., Abbott C.L. 2012. Molecular

977 phylogeny of *Gyrodactylus* (Monogenea) parasitizing fishes in fresh water, estuarine, and marine

978 habitats in Canada. Canadian J. Zool. 90: 776-786.

979 Gower J.C. 1975. Generalized procrustes analysis. Psychometrika 40: 33-51.

980 Graham J.H., Raz S., Hel-Or H., Nevo E. 2010. Fluctuating asymmetry: methods, theory and

981 applications. Symmetry 2: 466-540.

982 Grégoir A.F., Hablützel P.I., Vanhove M.P.M., Pariselle A., Bamps J., Volckaert F.A.M.,

983 Raeymaekers J.A.M. 2015. A link between host dispersal and parasite diversity in two sympatric

984 cichlids of Lake Tangayika. Freshwater Biol. 60: 323-335.

985 Hahn C., Weiss S.J., Stojanovski S., Bachmann L. (2015). Co-speciation of the ectoparasite

986 *Gyrodactylus teuchis* (Monogenea, Platyhelminthes) and its salmonid hosts. PLoS ONE 10:

987 e0127340.

988 Hahn C., Bakke T.A., Bachmann L., Weiss S., Harris P.D. 2011. Morphometric and molecular

989 characterization of *Gyrodactylus teuchis* Lautraite, Blanc, Thiery, Daniel & Vigneulle, 1999

990 (Monogenea: Gyrodactylidae) from an Austrian brown trout population. Parasitol. Int. 60: 480-

991 487.

992   Hayward C. 2005. Monogenea Polyopisthocotylea (ectoparasitic flukes). In: Rohde K., editor.

993   Marine Parasitology. Australia: CSIRO Publishing. p. 55-63.

994   Ho L.S.T., Ané C. 2014. A linear-time algorithm for Gaussian and non-Gaussian trait evolution

995   models. Syst. Biol. 63: 397-408.

996   Huyse T., Audenaert V., Volckaert F.A.M. 2003. Speciation and host-parasite relationships in the

997   parasite genus *Gyrodactylus* (Monogenea, Platyhelminthes) infecting gobies of the genus

998   *Pomatoschistus* (Gobiidae, Teleostei). Int. J. Parasitol. 33: 1679-1689.

999   Huyse T., Volckaert F.A. 2005. Comparing host and parasite phylogenies: *Gyrodactylus*

1000   flatworms jumping from goby to goby. Syst. Biol. 54: 710-718.

1001   Jarkovský J., Morand S., Šimková A., Gelnar M. 2004. Reproductive barriers between congeneric

1002   monogenean parasites (*Dactylogyrus*: Monogenea): attachment apparatus morphology or

1003   copulatory organ incompatibility? Parasitol. Res. 92: 95-105.

1004   Jolliffe I.T. 2002. Principal Component Analysis. 2nd ed. New York: Springer-Verlag.

1005   Kaci-Chaouch T., Verneau O., Desdevises Y. 2008. Host specificity is linked to intraspecific

1006   variability in the genus Lamellodiscus (Monogenea). Parasitol. 135: 607-616.

1007   Kahle D., Wickham H. 2013. ggmap: spatial visualization with ggplot2. The R Journal 5(1): 144-

1008   161.

1009   Kamilar J.M., Cooper N. 2013. Phylogenetic signal in primate behaviour, ecology and life

1010   history. Phil. Trans. R. Soc. B 368: 20120341.

1011   Katoh K., Standley D.M. 2013. MAFFT multiple sequence alignment software version 7:

1012   Improvements in performance and usability. Mol. Biol. Evol. 30: 772-780.

1013   Kearn G.C. 2014. Some aspects of the biology of monogenean (Platyhelminth) parasites of

1014   marine and freshwater fishes. Oceanography 2: 117. doi: 10.4172/2332-2632.1000117

1015   Khang T.F. 2015. monogeneaGM: geometric morphometric analysis of monogenean anchors. R

1016   package version 1.0. Available at: http://CRAN.R-project.org/package=monogeneaGM.

1017   Klingenberg C.P. 2008. Morphological integration and developmental modularity. Annu. Rev.

1018   Ecol. Evol. Syst. 39: 115-132.

1019   Klingenberg C.P. 2013. Visualizations in geometric morphometrics: how to read and how to make

1020   graphs showing shape changes. Hystrix 24:15–24.

1021   Klingenberg C.P., Ekau W. 1996. A combined morphometric and phylogenetic analysis of an

1022   ecomorphological trend: pelagization in Antarctic fishes (Perciformes: Nototheniidae). Biol. J.

1023   Linn. Soc. 59: 143-177.

1024   Koehn J.D., Crook D.A. 2013. Movement and migration. In: Humphries P., Walker K., editors.

1025   Ecology of Australian Freshwater Fishes. Australia: CSIRO Publishing. p. 105-130.

1026   Koskivaara M., Valtonen E.T., Vuori K-M. 1992. Microhabitat distribution and coexistence of

1027   *Dactylogyrus* species (Monogenea) on the gills of roach. Parasitology 104: 273-281.

1028   Kritsky D.C., Khamees N.R., Ali A.H. 2013. *Ligophorus* spp. (Monogenoidea: Dactylogyridae)

1029   parasitizing mullets (Teleostei: Mugiliformes: Mugilidae) occurring in the fresh and brackish

1030   waters of the Shatt Al-Arab River and Estuary in southern Iraq, with the description of

1031   *Ligophorus sagmarius* sp. n. from the greenback mullet *Chelon subviridis* (Valenciennes).

1032   Parasitol. Res. 112: 4029-4041.

1033 Lambert A., Maillard C. 1975. Repartition branchiale de deux monogenes: *Diplectanum aequans*

1034 (Wagener, 1857) Diesing, 1858 et *D. laubieri* Lambert A., Maillard, C., 1974 (Monogenea:

1035 Monopisthocotylea) parasites simultanes de *Dicentrarchus labrax* (Teleosteen). Ann. Parasitol.

1036 Hum. Comp. 50: 691-699.

1037 Lim L.H.S. 1991. Three new species of *Bychowskyella* Achmerow, 1952 (Monogenea) from

1038 Peninsular Malaysia. Syst. Parasitol. 19: 33-41.

1039 Lim L.H.S., Gibson D.I. 2009. A new monogenean genus from an ephippid fish off Peninsular

1040 Malaysia. Syst. Parasitol. 73: 13-25.

1041 Littlewood D.T.J. 2008. Platyhelminth systematics and the emergence of new characters. Parasite

1042 15: 333-341.

1043 Littlewood D.T.J., Olson P.D. 2001. Small subunit rDNA and the Platyhelminthes: Signal, noise,

1044 conflict and compromise. In: Littlewood D.T.J., Bray R.A., editors. Interrelationships of the

1045 Platyhelminthes. New York: Taylor & Francis. p. 262-278.

1046 Littlewood D.T.J., Rohde K., Clought K.A. 1997. Parasite speciation within or between host

1047 species? Phylogenetic evidence from site-specific polystome monogeneans. Int. J. Parasitol. 27:

1048 1289-1297.

1049 Llopis-Belenguer C., Balbuena J.A., Galván-Femenía I., Rodríguez-González A. 2015.

1050 Phenotypic buffering in a monogenean: canalization and developmental stability in shape and

1051 size of the haptoral anchors of *Ligophorus cephali* (Monogenea: Dactylogyridae). PLoS ONE 10:

1052 e0142365.

1053   Lockyer A.E., Olson P.D., Littlewood D.T.J. 2003. Utility of complete large and small subunit

1054   rRNA genes in resolving the phylogeny of the Neodermata (Platyhelminthes): implications and a

1055   review of the cercomer theory. Biol. J. Linn. Soc. 78: 155-171.

1056   Machkewskyi V.K., Dmitrieva E.V., Gibson D.I., Al-Jufaili S. 2014. *Lamellodiscus* aff. *euzeti*

1057   Diamanka, Boudaya, Toguebaye & Pariselle, 2011 (Monogenea: Diplectanidae) from the gills of

1058   *Cheimerius nufar* (Valenciennes) (Pisces: Sparidae) collected in the Arabian Sea, with comments

1059   on the distribution, specificity and historical biogeography of *Lamellodiscus* spp. Syst. Parasitol.

1060   89: 215-236.

1061   MacLeod N. 2013. Landmarks and semilandmarks: differences without meaning and meaning

1062   without differences. Available at: http://www.palass.org.

1063   Maddison W.P. 1997. Gene trees in species trees. Syst. Biol. 46: 523-536.

1064   Maechler M., Rousseeuw P., Struyf A., Hubert M., Hornik K. 2015. cluster: Cluster Analysis

1065   Basics and Extensions. R package version 2.0.2. Available at: https://cran.r-

1066   project.org/src/contrib/Archive/cluster/cluster_2.0.2.tar.gz.

1067   Marchiori N.C., Pariselle A., Pereira J., Agnese J.F., Durand J.D., Vanhove M.P. 2015. A

1068   comparative study of *Ligophorus uruguayense* and *L. saladensis* (Monogenea:

1069   Ancyrocephalidae) from *Mugil liza* (Teleostei: Mugilidae) in southern Brazil. Folia Parasitol. 62:

1070   024.

1071   Marcus L.F. 1990. Traditional morphometrics. In: Rohlf F.J., Bookstein F.L., editors. Proceedings

1072   of the Michigan Morphometrics Workshop. Ann Arbor, Michigan: University of Michigan

1073   Museums. p.77-122.

1074 Mariniello L., Ortis M., D'Amelio S., Petrarca V. 2004. Morphometric variability between and

1075 within species of *Ligophorus* Euzet & Suriano, 1977 (Monogenea: Ancyrocephalidae) in the

1076 Mediterranean Sea. Syst. Parasitol. 57: 183-190.

1077 Mendlová M., Šimková A. 2014. Evolution of host specificity in monogeneans parasitizing

1078 African cichlid fish. Parasit. Vectors 7: 69.

1079 Messu Mandeng F.D., Bilong Bilong C.F., Pariselle A., Vanhove M., Bitja Nyom A.R., Agnèse J.-

1080 F. 2015. A phylogeny of Cichlidogyrus spp. (Monogenea, Dactylogyridea) clarifies a host-switch

1081 between fish families and reveals an adaptive component to attachment organ morphology of this

1082 parasite genus. Parasite. Vector. 8: 582.

1083 Minh B.Q., Nguyen M.A.T., von Haeseler A. 2013. Ultrafast approximation for phylogenetic

1084 bootstrap. Mol. Biol. Evol. 30: 1188-1195.

1085 Mollaret I., Jamieson B.G.M., Justine J.-L. 2000. Phylogeny of the Monopisthocotylea and

1086 Polyopisthocotylea (Platyhelminthes) inferred from 28S rDNA sequences. Int. J. Parasitol. 30:

1087 11-185.

1088 Morand S., Šimková A., Matejusová I., Plaisance L., Verneau O., Desdevises Y. 2002.

1089 Investigating patterns may reveal processes: evolutionary ecology of ectoparasitic monogeneans.

1090 Int. J. Parasitol. 32: 111-119.

1091   Mouillot D., Šimková A., Morand S., Poulin R. 2005. Parasite species coexistence and limiting

1092   similarity: a multiscale look at phylogenetic, functional and reproductive distances. Oecologia

1093   146: 269-278.

1094   Mundry R. 2014. Statistical issues and assumptions of phylogenetic generalized least squares. In:

1095   Garamszegi L.Z., editor. Modern Phylogenetic Comparative Methods and Their Application in

1096   Evolutionary Biology. New York: Springer-Verlag. p. 131-153.

1097   Murray A.M. 2001. The fossil record and biogeography of the Cichlidae (Actinopterygii:

1098   Labroidei). Biol. J. Linn. Soc. 74: 517-532.

1099   Nieberding C.M., Olivieri I. 2007. Parasites: proxies for host genealogy and ecology? Trends

1100   Ecol. Evol. 22: 156-165.

1101   Nguyen L.-T., Schmidt H.A., von Haeseler A., Minh B.Q. 2015. IQ-TREE: A fast and effective

1102   stochastic algorithm for estimating maximum likelihood phylogenies. Mol. Biol. Evol. 32: 268-

1103   274.

1104   Olson E.C., Miller E.L. 1958. Morphological Integration. Chicago: University of Chicago Press.

1105   Öztürk T., Özer A. 2014. Monogenean fish parasites, their host preferences and seasonal

1106   distributions in the Lower Kizilirmak Delta (Turkey). Turk. J. Fish. Aquat. Sc. 14: 367-378.

1107   Paradis E., Claude J., Strimmer K. 2004. APE: Analyses of Phylogenetics and Evolution in R

1108   language. Bioinformatics 20: 289-290.

1109   Pariselle A., Boeger W.A., Snoeks J., Bilong Bilong C.F., Morand S., Vanhove M.P.M. 2011. The

1110   monogenean parasite fauna of cichlids: a potential tool for host biogeography. Int. J. Evol. Biol.

1111   2011: 471480.

1112 Perkins E.M., Donnellan S.C., Bertozzi T., Chisholm L.A., Whittington I.D. 2009. Looks can

1113 deceive: molecular phylogeny of a family of flatworm ectoparasites (Monogenea: Capsalidae)

1114 does not reflect current morphological classification. Mol. Phylogenet. Evol. 52: 705-714.

1115 Pepinelli M., Spironello M., Currie D.C. 2013. Geometric morphometrics as a tool for

1116 interpreting evolutionary transitions in the black fly wing (Diptera: Simuliidae). Zool. J. Linn.

1117 Soc. 169: 377-388.

1118 Pérez Ben C.M., Gómez R.O., Báez A.M. 2014. Intraspecific morphological variation and its

1119 implication in the taxonomic status of '*Bufo pisanoi*', a Pliocene anuran from eastern Argentina.

1120 J. Vertebr. Paleontol. 34: 767-777.

1121 Pfennig D.W., Wund M.A., Snell-Rood E.C., Cruickshank T., Schlichting C.D., Moczek A.P.

1122 2010. Phenotypic plasticity's impacts on diversification and speciation. Trends Ecol. Evol. 25:

1123 459-467.

1124 Pizzo A., Zagaria D., Palestrini C. 2013. An unfinished speciation process revealed by geometric

1125 morphometrics, horn allometries and biomolecular analyses: The case of the fracticornis-similis-

1126 opacicollis species complex of the genus *Onthophagus* (Coleoptera: Scarabaeidae). Zool. Anz.

1127 252: 548-561.

1128 Poisot T., Desdevises Y. 2010. Putative speciation events in *Lamellodiscus* (Monogenea:

1129 Diplectanidae) assessed by a morphometric approach. Biol. J. Linn. Soc. 99: 559-569.

1130 Poisot T., Verneau O., Desdevises Y. 2011. Morphological and molecular evolution are not linked

1131 in *Lamellodiscus* (Plathyhelminthes, Monogenea). PLoS ONE 6: e26252.

1132 Poulin R. 2002. The evolution of monogenean diversity. Int. J. Parasitol. 32: 245-254.

1133   R Core Team. 2015. R: A language and environment for statistical computing. R Foundation for

1134   Statistical Computing. Vienna, Austria. URL http://www/R-project.org/.

1135   Rae T.C. 1998. The logical basis for the use of continuous characters in phylogenetic systematics.

1136   Cladistics 14: 221-228.

1137   Raeymaekers J., Huyse T., Maelfait H., Hellemans B., Volckaert F. 2008. Community structure,

1138   population structure and topographical specialisation of *Gyrodactylus* (Monogenea) ectoparasites

1139   living on sympatric stickleback species. Folia Parasitol. 55: 187-196.

1140   Ramasamy P., Ramalingam K., Hanna R.E.B., Halton D.W. 1985. Microhabitat of gill parasites

1141   (Monogenea and Copepoda) of teleosts (*Scomberoides* spp.). Int. J. Parasitol. 15: 385-397.

1142   Reyment R.A., Blackith R.E., Campbell N.A. 1984. Multivariate Morphometrics. 2nd ed.

1143   London: Academic Press.

1144   Revell L.J. 2012. phytools: an R package for phylogenetic comparative biology (and other

1145   things). Methods Ecol. Evol. 3: 217-223.

1146   Revell L.J. 2014. Graphical methods for visualizing comparative data on phylogenies. In:

1147   Garamszegi L.Z., editor. Modern Phylogenetic Comparative Methods and Their Application in

1148   Evolutionary Biology. New York: Springer-Verlag. p. 77-104.

1149   Rodríguez-González A., Míguez-Lozano R., Llopis-Belenguer C., Balbuena J.A. 2015a.

1150   Phenotypic plasticity in haptoral structures of *Ligophorus cephali* (Monogenea: Dactylogyridae)

1151   on the flathead mullet (*Mugil cephalus*): a geometric morphometric approach. Int. J. Parasitol. 45:

1152   295-303.

1153   Rodríguez-González A., Míguez-Lozano R., Llopis-Belenguer C., Balbuena J.A. 2015b. A new

1154   species of *Ligophorus* (Monogenea: Dactylogyridae) from the gills of the flathead mullet *Mugil*

1155   *cephalus* (Teleostei: Mugilidae) from Mexico. Acta Parasitol. 60: 767-776.

1156   Rohde K. 1977. A non-competitive mechanism responsible for restricting niches. Zool. Anz. 199:

1157   164-172.

1158   Rohde K. 1979. A critical evalution of intrinsic and extrinsic factors responsible for niche

1159   restriction in parasites. Am. Nat. 114: 648-671.

1160   Rohde K. 1994. Niche restriction in parasites – proximate and ultimate causes. Parasitology 109:

1161   S69-S84.

1162   Rohde K., Watson N. 1985. Morphology, microhabitats and geographical variation of Kuhnia

1163   spp. (Monogenea: Polyopisthocotylea). Int. J. Parasitol. 15: 569-586.

1164   Rohde K., Hobbs R.P. 1986. Species segregation: competition or reinforcement of reproductive

1165   barriers? In: Cremin M., Dobson C., Noorhouse E., editors. Parasites Lives: Papers on Parasites,

1166   Their Hosts and Their Associations to Honour JFA Sprent. St. Lucia: University of Queensland

1167   Press. p.189-199.

1168   Rohde K., Hayward C., Heap M., Gosper D. (1994). A tropical assemblage of ectoparasites – gill

1169   and head parasites of *Lethrinus miniatus* (Teleostei, Lethrinidae). Int. J. Parasitol. 24: 1031-1053.

1170   Rohlf F.J. 2013. tpsDig, digitize landmarks and outliers, version 2.17. Department of Ecology

1171   and Evolution, State University of New York at Stony Brook.

1172   Rohlf F.J. 2015. The tps series of software. Hystrix. 26, doi: 10.4404/hystrix-26.1-11264.

1173   Rohlf F.J., Corti M. 2000. Use of two-block partial least-squares to study covariation in shape.

1174   Syst. Biol. 49: 740-753.

1175   Rohlf F.J., Marcus L.F. 1993. A revolution in morphometrics. Trends Ecol. Evol. 8: 129-132.

1176   Rohlf F.J., Slice D.E. 1990. Extensions of the Procrustes method for the optimal superimposition

1177   of landmarks. Syst. Zool. 39: 40-59.

1178   Roubal F.R. 1981. The taxonomy and site specificity of the metazoan ectoparasites on the black

1179   bream, *Acanthopagrus australis* (Günther), in northern New South Wales. Aust. J. Zool. 30: 1-

1180   100.

1181   Sanderson M.J., McMahon M.M., Steel M. 2010. Phylogenomics with incomplete taxon

1182   coverage: the limits to inference. BMC Evol. Biol. 10:155.

1183   Sarabeev V., Desdevises Y. 2014. Phylogeny of the Atlantic and Pacific species of *Ligophorus*

1184   (Monogenea: Dactylogyridae): morphology vs. molecules. Parasitol. Int. 63: 9-20.

1185   Shinn A.P., Gibson D.I., Sommerville C. 2001. Morphometric discrimination of *Gyrodactylus*

1186   *salaris* Malmberg (Monogenea) from species of *Gyrodactylus* parasitizing British salmonids

1187   using novel parameters. J. Fish Dis. 24: 83-97.

1188   Shinn A.P., Hansen H., Olstad K., Bachmann L., Bakke T.A. 2004. The use of morphometric

1189   characters to discriminate specimens of laboratory-reared and wild populations of *Gyrodactylus*

1190   *salaris* and *G. thymali* (Monogenea). Folia Parasitol. 51: 239:252.

1191   Sidlauskas B. 2008. Continuous and arrested morphological diversification in sister clades of

1192   characiform fishes: a phylomorphospace approach. Evolution 12: 3135-3156.

1193   Sidlauskas B.L., Mol J.H., Vari R.P. 2011. Dealing with allometry in linear and geometric

1194   morphometrics: a taxonomic case study in the *Leporinus cylindriformis* group (Characiformes:

1195   Anostomidae) with description of a new species from Suriname. Zool. J. Linn. Soc. 162: 103-

1196   130.

1197   Sievwright H., MacLeod N. 2012. Eigensurface analysis, ecology, and modelling of

1198   morphological adaptation in the falconiform humerus (Falconiformes: Aves). Zool. J. Linn. Soc.

1199   165: 390-419.

1200   Šimková A., Morand S. 2008. Co-evolutionary patterns in congeneric monogeneans: a review of

1201   *Dactylogyrus* species and their cyprinid hosts. J. Fish Biol. 73: 2210-2227.

1202   Šimková A., Rohde K. 2013. Community stability and instability in ectoparasites of marine and

1203   freshwater fish. In: Rohde K., editor. The Balance of Nature and Human Impact. Cambridge:

1204   Cambridge University Press. p. 75-88.

1205   Šimková A., Morand S. 2015. Parasite species coexistence and the evolution of the parasite niche.

1206   In: Morand S., Krasnov B.R., Littlewood D.T.J. editors. Parasite Diversity and Diversification.

1207   Cambridge: Cambridge University Press. p. 360-375.

1208   Šimková A., Ondračková M., Gelnar M., Morand S. 2002. Morphology and coexistence of

1209   congeneric ectoparasite species: reinforcement of reproductive isolation? Biol. J. Linn. Soc. 76:

1210   125–135.

1211   Šimková A., Verneau O., Gelnar M., Morand S. 2006. Specificity and specialization of

1212   congeneric monogeneans parazitizing cyprinid fish. Evolution 60: 1023–1037.

1213   Šimková A., Serbielle C., Pariselle A., Vanhove M.P.M., Morand S. 2013. Speciation in

1214   *Thaparocleidus* (Monogenea: Dactylogyridae) parasitizing Asian pangasiid catfishes. BioMed

1215   Res. Int. Article ID 353956. doi:10.1155/2013/353956.

1216   Siquier G.F., Ostrowski de Núñez M. 2009. Ligophorus uruguayense sp. Nov. (Monogenea,

1217   Ancyrocephalidae), a gill parasite from Mugil platanus (Mugiliformes, Mugilidae) in Uruguay.

1218   Acta Parasitol. 54: 95-102.

1219   Smith U.E., Hendricks J.R. 2013. Geometric morphometric character suites as phylogenetic data:

1220   extracting phylogenetic signal from gastropod shells. Syst. Biol. 62: 366-385.

1221   Soo O.Y.M., Lim L.H.S. 2012. Eight new species of *Ligophorus* Euzet & Suriano, 1977

1222   (Monogenea: Ancyrocephalidae) from mugilids off Peninsular Malaysia. Raffles Bull. Zool. 60:

1223   241-264.

1224   Soo O.Y.M., Lim L.H.S. 2015. A description of two new species of *Ligophorus* Euzet & Suriano,

1225   1977 (Monogenea: Ancyrocephalidae) from Malaysian mugilid fish using principal component

1226   analysis and numerical taxonomy. J. Helminthol. 89: 131-149.

1227   Soo O.Y.M., Tan W.B., Lim L.H.S. 2015. Three new species of *Ligophorus* Euzet & Suriano,

1228   1977 (Monogenea: Ancyrocephalidae) from *Moolgarda buchanani* (Bleeker) off Johor, Malaysia

1229   based on morphological, morphometric and molecular data. Raffles Bull. Zool. 63: 49-65.

1230   Sparks J.S., Smith W.L. 2005. Freshwater fishes, dispersal ability, and non-evidence: "Gondwana

1231   Life Rafts" to the rescue. Syst. Biol. 53: 11-19.

1232   Swofford D.L. 2002. PAUP: phylogenetic analysis using parsimony, Ver. 4.0.b10. Sunderland,

1233   Massachusetts: Sinaeur Associates.

1234 Tamura K., Stecher G., Pedersen D., Filipski A., Kumar S. 2013. MEGA 6: Molecular

1235 Evolutionary Genetics Analysis Version 6.0. Mol. Biol. Evol. 30: 2725-2729.

1236 Tan W.B. 2013. Morphological and molecular characterisation of monogeneans. Ph.D thesis,

1237 University of Malaya.

1238 Tan W.B., Khang T.F., Lim L.H.S. 2010. Morphometric analysis of *Trianchoratus* Price & Berry,

1239 1966 (Monogenea: Heteronchocleidinae) from *Channa* spp. (Osteichthyes: Channidae) of

1240 Peninsular Malaysia. Raffles Bull. Zool. 58: 165-172.

1241 Teo B.G., Sarinder K.K.S., Lim L.H.S. 2010. A novel alternative method for 3D visualisation in

1242 parasitology: the construction of a 3D model of a parasite from 2D illustrations. Trop. Biomed.

1243 27: 254-264.

1244 Teo B.G., Sarinder K.K.S., Lim L.H.S. 2013. A deformable generic 3D model of haptoral anchor

1245 of monogenean. PLoS ONE 8(10): e77650.

1246 Thiele K. 1993. The holy grail of the perfect character: the cladistic treatment of morphometric

1247 data. Cladistics 9: 275-304.

1248 van Valen L. 1965. Morphological variation and width of ecological niche. Am. Nat. 99: 377-390.

1249 Vanhove M.P.M., Huyse T. 2015. Host specificity and species jumps in fish-parasite systems. In:

1250 Morand S., Krasnov B.R., Littlewood D.T.J. editors. Parasite Diversity and Diversification.

1251 Cambridge: Cambridge University Press. p. 401-419.

1252 Vanhove M.P.M., Tessens B., Schoelinck C., Jondelius U., Littlewood D.T.J., Artois T., Huyse T.

1253 2013. Problematic barcoding in flatworms: A case-study on monogeneans and rhabdocoels

1254 (Platyhelminthes). ZooKeys 365: 355-379.

1255 Vanhove M.P.M., Pariselle A., Van Steenberge V., Raeymaekers J.A.M., Hablützel P.I., Gillardin

1256 C., Hellemans B., Breman F.C., Koblmüller S., Sturmbauer C., Snoeks J., Volckaert F.A.M.,

1257 Huyse T. 2015. Hidden biodiversity in an ancient lake: phylogenetic congruence between Lake

1258 Tanganyika tropheine cichlids and their monogenean flatworm parasites. Sci. Rep. 5: 13669.

1259 Vignon M. 2011. Putting in shape – towards a unified approach for the taxonomic description of

1260 monogenean haptoral hard parts. Syst. Parasitol. 79: 161-174.

1261 Vignon M., Sasal P. 2010. The use of geometric morphometrics in understanding shape

1262 variability of sclerotized haptoral structures of monogeneans (Platyhelminthes) with insights into

1263 biogeographic variability. Parasitol. Int. 59: 183-191.

1264 Vignon M., Pariselle A., Vanhove M.P.M. 2011. Modularity in attachment organs of African

1265 *Cichlidogyrus* (Platyhelminthes: Monogenea: Ancyrocephalidae) reflects phylogeny rather than

1266 host specificity or geographic distribution. Biol. J. Linn. Soc. 102: 694-706.

1267 Waeschenbach A., Webster B.L., Bray R.A., Littlewood D.T.J. 2007. Added resolution among

1268 ordinal level relationships of tapeworms (Platyhelminthes: Cestoda) with complete small and

1269 large subunit nuclear ribosomal RNA genes. Mol. Phylogenet. Evol. 45: 311-325.

1270 Warnes G.R., Bolker B., Bonebakker L., Gentleman R., Huber W., Liaw A., Lumley T., Maechler

1271 M., Magnusson A., Moeller S., Scharwtz M., Venables B. 2014. gplots: various R programming

1272 tools for plotting data. R package version 2.13.0. Available at: http://CRAN.R-

1273 project.org/pacakge=gplots.

1274 Werneburg I., Wilson L.A.B., Parr W.C.H., Joyce W.G. 2015. Evolution of neck vertebral shape

1275 and neck retraction at the transition to modern turtles: an integrated geometric morphometric

1276 approach. Syst. Biol. 64: 187-204.

1277   Wheeler Q.D. 2007. Digital innovation and taxonomy's finest hour. In: MacLeod N., editor.

1278   Automated Taxon Identification in Systematics: Theory, Approaches and Applications. Boca

1279   Raton: CRC Press. p. 9-23.

1280   Whittington I.D. 2005. Monogenea Monopisthocotylea (ectoparasitic flukes). In: Rohde K.,

1281   editor. Marine Parasitology. Australia: CSIRO Publishing. p. 63-72.

1282   Whittington I.D., Cribb B.W., Hamwood T.E., Halliday J.A. 2000. Host-specificity of

1283   monogenean (platyhelminth) parasites: a role for anterior adhesive areas? Int. J. Parasitol. 30:

1284   305-320.

1285   Whittington I.D., Kearn G.C. 2011. Hatching strategies in monogenean (platyhelminth) parasites

1286   that facilitate host infection. Integr. Comp. Biol. 51: 91-99.

1287   Wiens J.J. 2001. Character analysis in morphological phylogenetics: problems and solutions.

1288   Syst. Biol. 50: 689-699.

1289   Wilkinson L., Friendly M. 2008. The history of the cluster heat map. Am. Stat. 63: 179-184.

1290   Wong W.L., Gorb S.N. 2013. Attachment ability of a clamp-bearing fish parasite, *Diplozoon*

1291   *paradoxum* (Monogenea) on gills of the common bream *Abramis brama*. J. Exp. Biol. 216: 3008-

1292   3014.

1293   Yang Z. 2006. Computational Molecular Evolution. Oxford, UK: Oxford University Press.

1294   Zietara M.S., Lumme J. 2002. Speciation by host switch and adaptive radiation in a fish parasite

1295   genus *Gyrodactylus* (Monogenea, Gyrodactylidae). Evolution 56: 2445-2458.

1296   FIGURE CAPTIONS

1297 FIGURE 1. a) Landmarks of the i) ventral and ii) dorsal anchors of a *L. navjotsodhii* sample,

1298 digitized using TPSDIG2 (Version 2.17). The iii) ventral and iv) dorsal bars can also be seen in

1299 the image. b) Landmark positions on an anchor. Type I landmarks

1300 (LM1,LM2,LM3,LM5,LM7,LM8) are indicated by stars, while Type III landmarks

1301 (LM4,LM6,LM9,LM10,LM11) are indicated by solid circles. Abbreviations: ORP - outer root

1302 point; GP - groove point; IRP - inner root point; DP - dent point; CP - curve point; TP - tip point.

1303 FIGURE 2. Wireframe plots of anchors of *L. navjotsodhii* lying in their natural positions in the

1304 mounted slide. a) Example of a poor quality specimen (Q = 5); note the larger than expected

1305 variation between shape of (larger) left and right forms of the dorsal anchors, which shows up in

1306 a Tukey Mean Difference (TMD) plot that has relatively wide width of 95% limits of agreement

1307 (upper and lower dashed lines) as well as a fanning pattern as A becomes larger. b) Example of a

1308 good quality specimen (Q=30); note the lack of shape variation between left and right forms of

1309 ventral and dorsal anchors, which shows up in a TMD plot with much narrower width of 95%

1310 limits of agreement as well as a more or less random deviation of M about 0 independent of A.

1311 FIGURE 3. Molecular phylogeny of the 13 *Ligophorus* species inferred using the maximum

1312 likelihood method (10000 bootstrap replicates) with annotations from three anatomical structures:

1313 anchors, bars and male copulatory organ (30% of original scale). Species in Clade I are found in

1314 *Moolgarda buchanani*, and species in Clade II are found in *Liza subviridis*. The ventral and

1315 dorsal forms of the anchors are arranged from left to right, those of the bars from top to bottom.

1316 FIGURE 4. Scatter plots of Generalized Procrustes Analysis coordinates of all specimens for the

1317 a) ventral anchors and b) dorsal anchors. The species centroids of each landmark are indicated by

1318 solid, colored circles.

1319   FIGURE 5. PCA plots of PC1 against PC2 and PC3 for a) ventral and b) dorsal anchors, with

1320   superimposed phylogeny of the 13 *Ligophorus* species. The centroids of the species are indicated

1321   in solid colors, while individual samples are plotted in high transparency colors. The estimated

1322   principal component coordinates of the ancestral nodes are represented by small open circles.

1323   FIGURE 6. Cluster heat map of specimens (column) using shape variable data (row). The name

1324   of a shape variables consists of three parts: a prefix indicating ventral (V) or dorsal (D) anchors, a

1325   number indicating landmark index, and a suffix indicating x or y coordinate value. a) Cluster heat

1326   map using filtered specimens with quality score of 10 or more (n=437); b) Cluster heat map using

1327   all specimens (n=530).

1328   FIGURE 7. Wireframe-lollipop plots of mean shape change relative to estimated ancestral mean

1329   shape in a) ventral anchors of Clade I (purple); b) dorsal anchors of Clade I; c) ventral anchors of

1330   Clade II (blue); d) dorsal anchors of Clade II. The p-value of Rayleigh test for uniform direction

1331   change at each landmark is indicated as a colored solid circle. The color bar maps color tones to

1332   their corresponding p-values.

1333   FIGURE 8. Scatter plots LM1-LM5 distance against LM1-LM3 distance for a) ventral and b)

1334   dorsal anchors. The dashed lines are cut-offs on the x and y axes that allow complete

1335   discrimination of Clade I from Clade II. Scatter plots of outer length (OL) against inner length

1336   (IL) for c) ventral and d) dorsal anchors. No cut-offs on the x and y axes permit complete

1337   discrimination of Clade I from Clade II.

1338   FIGURE 9. Continuous character mapping of anchor size (in μm) of ventral (left) and dorsal

1339   (right) anchors onto the maximum likelihood phylogeny of the 13 *Ligophorus* species.

1340   FIGURE 10. Scatter plot of male copulatory organ tube length against dorsal anchor shape. The

1341   size of dorsal anchors is proportional to the circle diameter. When anchor size and shape are

1342   similar, species that have similar size for the male copulatory organ show variation in the latter's

1343   morphology (I and II), whereas those with similar morphology of male copulatory organ show

1344   variation in the latter's size (III).

1345   FIGURE 11. Color-coded morphological character state data for the 13 *Ligophorus* species and

1346   their estimated maximum parsimony phylogeny (1000 bootstrap replicates). a) Result using the

1347   set of morphological characters (7 to 12) that contain discretized LM1-LM3 and LM1-LM5

1348   distances and anchor shaft shape. b) Result using anchor morphological characters derived from

1349   traditional morphometrics in Sarabeev and Desdevises (2014).

1350   TABLE CAPTIONS

1351   TABLE 1. GenBank accession numbers of 28S rRNA, 18S rRNA and ITS1 sequences of the 13

1352   *Ligophorus* species, with information about the latters' host species and collection location.

1353   Sequences obtained in present study are marked with an asterisk.

1354   TABLE 2. List of morphological characters used to construct maximum parsimony trees. All

1355   characters in Set B were taken from Sarabeev and Desdevises (2014). Characters 1-6 of Set B are

1356   the same as Set A's; Characters 7-12 of Set A were constructed in the present study based on

1357   results of geometric morphometric analysis.